ปริมาณรังสีและคุณภาพของภาพที่เหมาะสมในการถ่ายภาพรังสีทรวงอก ด้วยเครื่องเอกซเรย์เคลื่อนที่ระบบดิจิตอลของโรงพยาบาลจุฬาลงกรณ์

นายปิยทัศน์ แสงดาว

วิทยานิพนธ์นี้เป็นส่วนหนึ่งของการศึกษาตามหลักสูตรปริญญาวิทยาศาสตรมหาบัณฑิต
สาขาวิชาฉายาเวชศาสตร์ ภาควิชารังสีวิทยา
คณะแพทยศาสตร์ จุฬาลงกรณ์มหาวิทยาลัย
ปีการศึกษา 2557

OPTIMIZATION OF RADIATION DOSE AND IMAGE QUALITY IN CHEST RADIOGRAPHY USING DIGITAL MOBILE X-RAY SYSTEM AT KING CHULALONGKORN MEMORIAL HOSPITAL

Mr. Piyatas Sangdao

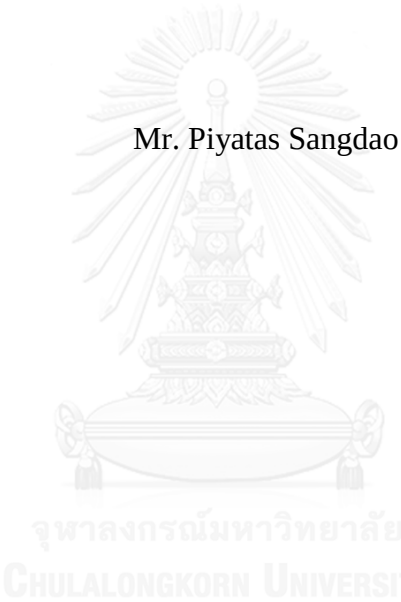

A Thesis Submitted in Partial Fulfillment of the Requirements
for the Degree of Master of Science Program in Medical Imaging
Department of Radiology
Faculty of Medicine
Chulalongkorn University
Academic Year 2014

Thesis Title	OPTIMIZATION OF RADIATION DOSE AND IMAGE QUALITY IN CHEST RADIOGRAPHY USING DIGITAL MOBILE X-RAY SYSTEM AT KING CHULALONGKORN MEMORIAL HOSPITAL
By	Mr. Piyatas Sangdao
Field of Study	Medical Imaging
Thesis Advisor	Associate Professor Anchali Krisanachinda, Ph.D.
Thesis Co-Advisor	Kitiwat Khamwan, Ph.D.

Accepted by the Faculty of Medicine, Chulalongkorn University in Partial Fulfillment of the Requirements for the Master's Degree

.....Dean of the Faculty of Medicine
(Associate Professor Sophon Napathorn, M.D.)

THESIS COMMITTEE

.....Chairman
(Associate Professor Kiat Arjhansiri, M.D.)

.....Thesis Advisor
(Associate Professor Anchali Krisanachinda, Ph.D.)

.....Thesis Co-Advisor
(Kitiwat Khamwan, Ph.D.)

.....External Examiner
(Professor Franco Milano, Ph.D.)

ปิยทัศน์ แสงดาว : ปริมาณรังสีและคุณภาพของภาพที่เหมาะสมในการถ่ายภาพรังสีทรวงอกด้วยเครื่องเอกซเรย์เคลื่อนที่ระบบดิจิตอลของโรงพยาบาลจุฬาลงกรณ์ (OPTIMIZATION OF RADIATION DOSE AND IMAGE QUALITY IN CHEST RADIOGRAPHY USING DIGITAL MOBILE X-RAY SYSTEM AT KING CHULALONGKORN MEMORIAL HOSPITAL) อ.ที่ปรึกษาวิทยานิพนธ์หลัก: รศ. ดร.อัญชลี กฤษณจินดา, อ.ที่ปรึกษาวิทยานิพนธ์ร่วม: อ. ดร.กิติวัฒน์ คำวัน, 89 หน้า.

ปัจจุบันเครื่องเอกซเรย์ระบบดิจิตอล เป็นเทคโนโลยีที่ทันสมัยและมีการนำมาใช้งานกันอย่างแพร่หลายในงานด้านรังสีวิทยาของฝ่ายรังสีวิทยาโรงพยาบาลจุฬาลงกรณ์ โดยมีการนำเครื่องเอกซเรย์เคลื่อนที่ระบบดิจิตอลมาใช้ในการให้บริการผู้ป่วยในหอพักผู้ป่วยซึ่งไม่สามารถเคลื่อนย้ายเพื่อมารับบริการที่ฝ่ายรังสีวิทยาได้ เมื่อเดือนกันยายน พ.ศ. 2556 การถ่ายภาพรังสีทรวงอกเป็นการตรวจที่แพทย์สั่งตรวจมากที่สุด และในบางรายมีการสั่งตรวจหลายครั้งในช่วงที่ทำการรักษาอยู่ในโรงพยาบาล ทำให้ผู้ป่วยมีโอกาสได้รับปริมาณรังสีมากขึ้นตามไปด้วย เครื่องถ่ายภาพรังสีระบบดิจิตอลใช้ปริมาณรังสีในการถ่ายภาพรังสีน้อยกว่าระบบซีอาร์และระบบเดิม ซึ่งนำไปสู่การเปลี่ยนแปลงค่าเทคนิคที่ใช้ในการถ่ายภาพรังสีให้เหมาะสม วัตถุประสงค์ของงานวิจัยนี้เพื่อศึกษาความเหมาะสมระหว่างปริมาณรังสีที่ผู้ป่วยได้รับกับคุณภาพของภาพรังสีทรวงอกที่ถ่ายภาพด้วยเครื่องเอกซเรย์เคลื่อนที่ระบบดิจิตอล ด้วยเลือกใช้ค่าเทคนิคต่างๆ โดยจะทำการศึกษาจากหุ่นจำลองก่อนเพื่อดูความสัมพันธ์ระหว่างค่าปริมาณรังสีที่ผิวของหุ่นจำลองได้รับกับคุณภาพของภาพซึ่งประเมินจากจำนวนองค์ประกอบของภาพรังสีทรวงอกตามมาตรฐานของคณะกรรมาธิการประชาคมยุโรป และระดับของสัญญาณรบกวน โดยผู้ประเมินผล 3 ท่าน จากนั้นจึงเลือกค่าเทคนิคที่เหมาะสมทั้งค่าปริมาณรังสีที่ผิวและคุณภาพของภาพ เพื่อนำใช้กับผู้ป่วยต่อไป

ผลของงานวิจัยนี้พบว่าค่าเทคนิคที่เหมาะสมสำหรับการถ่ายภาพรังสีทรวงอกโดยเครื่องเอกซเรย์เคลื่อนที่ระบบดิจิตอลของโรงพยาบาลจุฬาลงกรณ์ คือ ค่าเควีพี 90 และค่าเอ็มเอเอส 0.63 สำหรับผู้ป่วยที่มีความหนาของทรวงอกน้อยกว่าหรือเท่ากับ 23 เซนติเมตร นำไปใช้กับผู้ป่วยจำนวน 50 คน โดยคำนวณค่าปริมาณรังสีที่ผิวตามความหนาของทรวงอกผู้ป่วยและการประเมินคุณภาพของภาพโดยผู้ประเมิน พบว่าปริมาณรังสีที่ผิวของผู้ป่วยโดยเฉลี่ยมีค่า 0.076 มิลลิเกรย์ โดยผู้ป่วยมีความหนาของทรวงอกเฉลี่ย 19.70 เซนติเมตร คะแนนขององค์ประกอบของภาพรังสีทรวงอก พบว่าร้อยละ 88 ของภาพทั้งหมดมีค่ามากกว่าหรือเท่ากับ 3 โดยค่าที่ยอมรับได้อยู่ในช่วง 3 ถึง 6 คะแนน, ร้อยละ 70 ของภาพทั้งหมดมีคะแนนของระดับสัญญาณรบกวนเท่ากับ 2 และ ร้อยละ 30 ของภาพทั้งหมดมีคะแนนของระดับสัญญาณรบกวนเท่ากับ 3โดยค่าที่ยอมรับได้อยู่ในช่วง 2 ถึง 3 เมื่อเปรียบเทียบกับค่าปริมาณรังสีที่ผิวของผู้ป่วยก่อนทำการศึกษา ซึ่งมีค่าเฉลี่ย 0.192 มิลลิเกรย์ พบว่าปริมาณรังสีที่ผิวของผู้ป่วยจากการใช้ค่าเทคนิคที่เหมาะสมจากการวิจัยนี้ มีค่าลดลงร้อยละ 60 และปริมาณรังสียังมีค่าต่ำกว่าระดับรังสีอ้างอิงที่ทบวงการพลังงานปรมาณูระหว่างประเทศกำหนดไว้ที่ 0.4 มิลลิเกรย์

ภาควิชา รังสีวิทยา	ลายมือชื่อนิสิต .....
สาขาวิชา ฉายาเวชศาสตร์	ลายมือชื่อ อ.ที่ปรึกษาหลัก .....
ปีการศึกษา 2557	ลายมือชื่อ อ.ที่ปรึกษาร่วม .....

5674047730 : MAJOR MEDICAL IMAGING

KEYWORDS: CHEST RADIOGRAPH / ESAK / IMAGE QUALITY / NOISE / EXPOSURE PARAMETER

PIYATAS SANGDAO: OPTIMIZATION OF RADIATION DOSE AND IMAGE QUALITY IN CHEST RADIOGRAPHY USING DIGITAL MOBILE X-RAY SYSTEM AT KING CHULALONGKORN MEMORIAL HOSPITAL. ADVISOR: ASSOC. PROF. ANCHALI KRISANACHINDA, Ph.D., CO-ADVISOR: KITIWAT KHAMWAN, Ph.D., 89 pp.

Digital Radiography (DR) has become an important imaging modality at Department of Radiology, King Chulalongkorn Memorial Hospital. In September 2013, the digital mobile x-ray system has been in service on the patient ward for patients who could not move to the Department of Radiology. Chest radiography is the most common examination performed on the patient ward. Some patient was exposed several times during treatment, result in increasing the radiation dose. As the DR produces less patient radiation dose than the CR and conventional radiograph, the exposure parameters use for DR must be determined. The purpose of this study is to optimize the radiation dose and image quality for digital mobile chest radiography. Lung Phantom was firstly used to study the appropriate exposure parameters to optimize the radiation dose at surface of the phantom and image quality based on the Commission of European Communities (CEC) and the qualitative noise evaluated by three observers. The exposure parameters obtained will be further used for patients.

The proper exposure parameter for chest radiography was kVp 90 and mAs 0.63 for the patient chest thickness equal to or less than 23 cm. 50 patients were exposed by optimal parameters, then the patient dose had been calculated and the image quality has been assessed by three observers. The average patient dose was 0.076 mGy and the average of patient chest thickness was 19.70 cm. 88% of the images showed the image criteria score equal to or more than 3 where the acceptable score range from 3 to 6, 70% and 30% of the images showed the qualitative noise scores was 2 and 3 respectively where the acceptable score range from 2 to 3. The patient dose for routine chest study was 0.192 mGy. Therefore, the patient dose using optimal protocol was 60% less than routine study and also lower than the International Atomic Energy Agency dose reference level of 0.4 mGy for chest radiography.

Department:	Radiology	Student's Signature	.....
Field of Study:	Medical Imaging	Advisor's Signature	.....
Academic Year:	2014	Co-Advisor's Signature	.....

ACKNOWLEDGEMENTS

I would like to express sincere thanks and deepest appreciation to Associate Professor Anchali Krisanachinda, Ph.D., Department of Radiology, Faculty of Medicine, Chulalongkorn University, my advisor for her helpful, suggestion, supervision, guidance, constructive direction and polishing of the thesis writing to improve the English expression.

I would like to express sincere thanks to Mr. Kitiwat Khamwan, Ph.D., Department of Radiology, Faculty of Medicine, Chulalongkorn University, my co-advisor for his helpful, suggestion, supervision, guidance, and constructive direction in this research.

I would like to extremely thank Associate Professor Sivalee Suriyapee, M.Eng., Division of Radiation Oncology, Department of Radiology, Faculty of Medicine, Chulalongkorn University, my teacher for her suggestion, invaluable guidance, constructive direction and encouragement.

I would like to deeply thank Associate Professor Kiat Arjhansiri, M.D., Department of Radiology, Faculty of Medicine, Chulalongkorn University, Chairman of thesis defense for his suggestion, invaluable advices and constructive comments.

I would like to deeply thank Professor Franco Milano, Ph.D., University of Florence Italy, an external examiner of thesis defense for his helpful recommendations, constructive comments and teaching in Medical Imaging.

I would like to thank Ms. Petcharleeya Suwanpradit, M.Sc., Department of Radiology, King Chulalongkorn Memorial Hospital, for her guidance of using equipment, facilitating on protocol in this research, useful advices and encouragement.

I am extremely grateful for all teachers, lecturers and staff at Master of Science Program in Medical Imaging, Faculty of Medicine, Chulalongkorn University, for their help and unlimited knowledge during the course in Medical Imaging.

Finally, I am greatly thankful to my family for their invaluable encouragement, care and understanding during the entire course of the study.

CONTENTS

Page

Page

Page

Page

LIST OF TABLES

Table **Page**

LIST OF FIGURES

Figure **Page**

LIST OF ABBREVIATIONS

AAPM	American Association of Physicists in Medicine
ALARA	As Low As Reasonably Achievable
AP	Anterio-Posterior
BSF	Back Scatter Factor
CCD	Charge-Coupled Device
CEC	Commission of the European Communities
CNR	Contrast to Noise Ratio
CR	Computed Radiography
CXR	Chest Radiography
DQE	Detective Quantum Efficiency
DR	Digital Radiography
DRL	Dose Reference Level
ESAK	Entrance Surface Air KERMA
FID	Focus to Image receptor Distance
HVL	Half Value Layer
IAEA	International Atomic Energy Agency
ICU	Intensive Care unit
KCARE	King's Center for the Assessment of Radiological Equipment
kVp	Kilo Voltage Peak
mAs	MilliAmpere-Second
mGy	MilliGray
MTF	Modulation Transfer Function
NPS	Noise Power Spectrum
PA	Posterio-Anterior
PACS	Picture Archiving and Communication System
QA	Quality Assurance
QC	Quality Control
ROI	Region Of Interest
TFT	Thin-Film Transistor

CHAPTER 1
INTRODUCTION

1.1 Background and rationale

Digital imaging was firstly introduced in 1977 and put to clinical use in 1980. Digital imaging is currently used in practice to include both computed radiography and digital radiography(1).

Computed radiography (CR) replaced film by a storage phosphor plate as the image receptor. The latent image on the exposed plate is scanned by a laser beam and converted to digital data to produce the image(1).

Digital radiography (DR) involves collecting image data in digital format, without laser scanning to extract the latent image. The direct capture of x-rays for digital images was introduced with DR using a charge-coupled device (CCD) in 1990. The technology evolved and improved over the decade by 2001. Flat-panel thin-film transistor (TFT) detectors are exposed and display images in nearly real time. Future from CCD, current technology includes a variety of devices and materials such as photoconductors and x-ray scintillators in digital radiography(1).

The range of radiation dose that digital image receptors can detect has allowed wider values to be processed digitally to display a diagnostic quality image in comparison to screen film system (figure 1.1). The digital image has original, raw data that should be kept intact. Post-processing can change the original raw data and the set point that establishes the levels of gray scale assigned to the pixels. A change in the raw data can loss information in the PACS system (1) and affect the viewing capabilities.

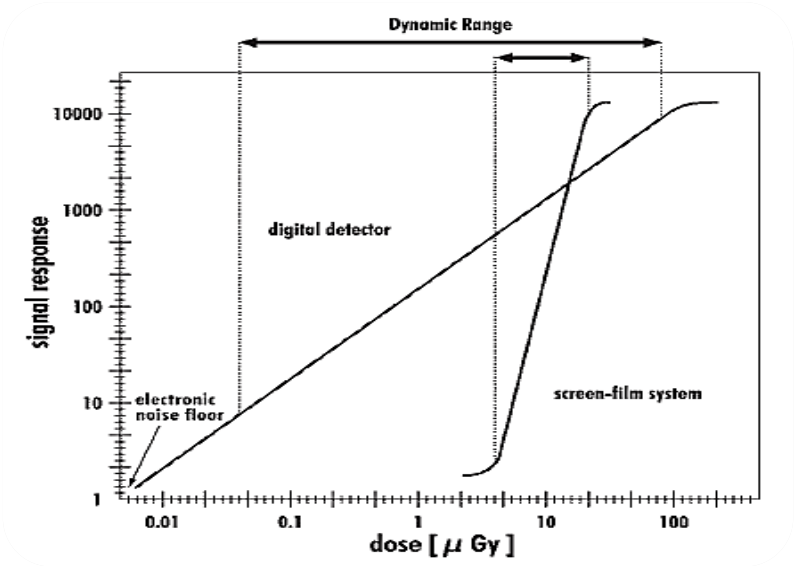

Figure 1.1 The dynamic range of digital detector and characteristic curve of screen-film system(2).

A mobile DR system used in this study was introduced to King Chulalongkorn Memorial Hospital in September 2013. There is an immediate read-out for visual control of image quality but suffers from a relatively bulky read-out unit to be managed within the patient room. Direct conversion systems use a photo conducting layer (amorphous selenium, a-Se), in which the absorbed x-ray energy is directly converted into charge on top of a TFT array. These systems offer the high spatial frequencies, absorb less x-ray energy, compared to CR or film-screen system. Based on this principle, the exposure parameters used in the CR or film-screen system should not be applied to DR system. They should be determined to optimize the patient radiation doses with the accepted image quality.

Optimization used in diagnostic radiologic imaging, is a balance between the benefit of the diagnostic imaging for the patient and the associated risk of the ionizing radiation exposure.

When following the ALARA principle, patient exposure could be minimized from digital radiography procedures. Using digital image receptors require careful and consistent attention to system protocol and practice standards. Digital radiography system separates acquisition, processing and display. The best practice is to select the

appropriate exposure technique factors for the patient size and condition, to obtain adequate image quality for diagnosis(1).

The chest radiography is requested for an immobilized patient using the mobile DR system more than any other examination in the department. The patients are unable coming to the department for routine chest PA radiography(2).

The chest radiography on the patient wards is essential to the process of medical treatment which may be taken several times throughout the period of treatment resulting in the radiation risk. Furthermore, the hospital staff including physician, nurses and other patients could receive scattered radiation from mobile chest radiography. Most patient wards are not specifically designed for radiation protection, therefore, the selection of the appropriate parameter for digital chest radiography could reduce the patient, staff and public radiation doses.

1.2 Objective

The objective of the study is to optimize the radiation dose and image quality for chest radiograph using digital mobile x-ray system at King Chulalongkorn Memorial Hospital.

1.3 Definition

Back Scatter Factor (BSF): The ratio between dose quantities measured at a phantom or material surface facing the source of radiation and the same dose quantity at the same position free in air.

Dose: Absorbed dose is the energy imparted to matter per unit mass of the irradiated matter. Absorbed dose is expressed in SI units of joule/kg (J/kg), non SI unit of rad or Gray (Gy).

Entrance Surface Air KERMA (ESAK): Absorbed dose in air at the center of the field at the patient surface including backscatter.

Exposure: A radiation quantity of charge produced by ionization in air from x-rays or gamma rays. Unit is expressed in coulomb per kilogram of air (C/kg), and non SI unit is Roentgen (R).

CHAPTER 2
LITERATURE REVIEW

2.1 Theory

2.1.1 Introduction

The bedside chest x-rays (CXR) is one of the most commonly requested examinations, and remains the cornerstone of diagnosis and monitoring of the intensive care unit (ICU) patient. Bedside CXR is essential for detecting malposition of monitor material, for identifying associated complications, and for analyzing the underlying reasons for cardiopulmonary deterioration(3).

The limitations of beside CXR are the superposition of soft tissue, pleural and pulmonary disease, as well as tubes and lines. Frequently, the patient is difficult to position, or is unable to cooperate, and the technical equipment is limited(3).

2.1.2 Digital Radiography

Digital radiography (DR) flat-panel systems with integrated readout mechanisms were introduced at the end of the 1990s (4). Flat-panel systems, large area x-ray detectors, integrate an x-ray sensitive layer and an electronic readable system based on TFT arrays are called direct conversion TFT detectors (4). A scintillator layer and a light-sensitive TFT photodiode had been used as an indirect conversion TFT detectors. The amorphous silicon (a-Si) used in TFT arrays to record the electronic signal is different from an amorphous selenium (a-Se) to capture x-ray energy in a direct digital detector. The structure of a DR flat-panel system is shown in figure 2.1.

This electronic readable system allows an active readout process, also called active matrix readout, in opposition to the storage-phosphor systems where no active readout elements are integrated within the detector. The entire readout process is very fast, allowing further developments in digital real-time x-ray detectors (4).

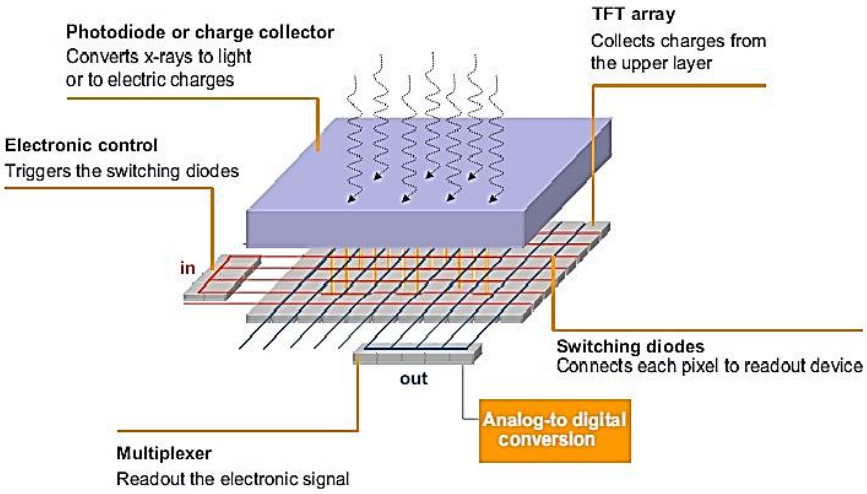

Figure 2.1 Flat-panel system structures (5).

TFT arrays (Figure 2.2) are typically deposited onto a glass substrate in multiple layers, with readout electronics at the lowest level, and charge collector arrays at higher levels. Depending on the type of detector being manufactured, charge collection electrodes or light sensing elements are deposited at the top layer of the ‘‘electronic sandwich’’(5).

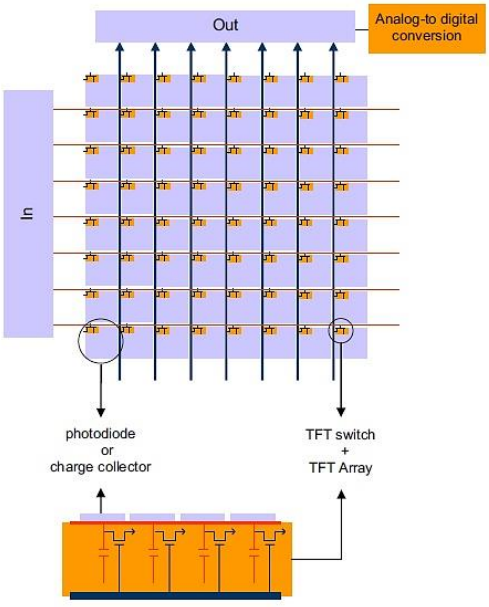

Figure 2.2 TFT array(5).

Large area direct conversion systems use amorphous selenium (a-Se) as the semiconductor material because of its x-ray absorption properties and extremely high intrinsic spatial resolution (4, 5). Before the flat-panel is exposed to x-rays an electric field is applied across the selenium layer. Then the x-ray exposure generates electrons and holes within the a-Se layer: the absorbed x-ray photons are transformed into electric charges and drawn directly to the charge-collecting electrodes due to the electric field. Those charges proportional to the incident x-ray beam are generated and migrate vertically to the both surfaces of the selenium layer, without much lateral diffusion. At the bottom of the a-Se layer, charges are drawn to the TFT charge collector, where they are stored until readout. The charge collected at each storage capacitor is amplified and quantified to a digital code value for the corresponding pixel. During the readout, the charge of the capacitors of every row is conducted by the transistors to the amplifiers.

Large area indirect conversion systems use cesium iodide (CsI) or gadolinium oxysulphide (Gd_2O_2S) as an x-ray detector. The scintillators and phosphors can be either structured or unstructured (Figure 2.3). Unstructured scintillators scatter a large amount of light and this reduces spatial resolution(4). Structured scintillators consist of phosphor material in a needlelike structure (the needles being perpendicular to the screen surface). This increases the number of x-ray photon interactions and reduces the lateral scattering of light photons(4).When the scintillator layer is exposed to x-rays the beam is absorbed and converted into fluorescent light. At a second stage that light is converted into an electric charge by means of an a-Si photodiode array(6). Indirect conversion detectors are constructed by adding an a-Si photodiode circuitry and a scintillator as the top layers of the TFT sandwich. These layers replace the x-ray semiconductor layer used in a direct conversion device(5). The active area of the detector is divided into an integrated array of image elements-the pixel-and each element contains a photodiode and a TFT switch available for the readout process.

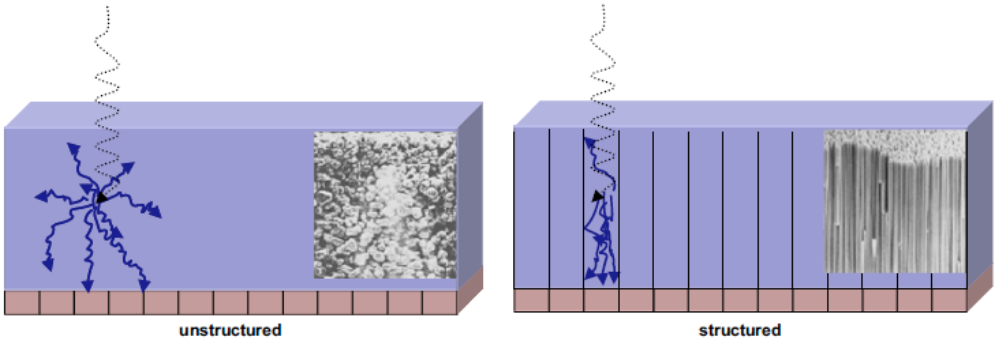

Figure 2.3 Schematic of an unstructured (left) and structured scintillator (right)(5).

Recent development for a novel pixel–structured scintillation screen with nanocrystalline Gd_2O_3: Eu particle size for high-spatial-resolution x-ray imaging detectors are being made for indirect x-ray imaging sensors with high sensitivity and high spatial resolution(7).

2.1.3 Post Processing

After exposure and readout, the raw imaging data is processed for display on the computer (Figure 2.4). Image processing improves image quality by reducing noise, removing technical artifacts, and optimizing contrast for viewing.

Altering processing features on digitally acquired images is not trivial. If one feature is being improved, others may be suppressed, so that unintended and unwanted masking of diagnostically relevant features may occur. Consequently, image processing must be optimized carefully for each digital radiography system. In addition, processing algorithms must be adapted to each anatomic region-meaning, for example, that different standards are required for lateral and postero-anterior chest radiography.

Image processing software is usually bundled with the detector and cannot be replaced by other software. In general, this arrangement allows processing algorithms to be optimized for a specific detector but does not rule out the possibility that use of a different processing software package might improve image quality even further.

Digital images consist of picture elements, or pixels. The two-dimensional collection of pixels in the image is called the matrix, which is usually expressed as length (in pixels) by width (in pixels).

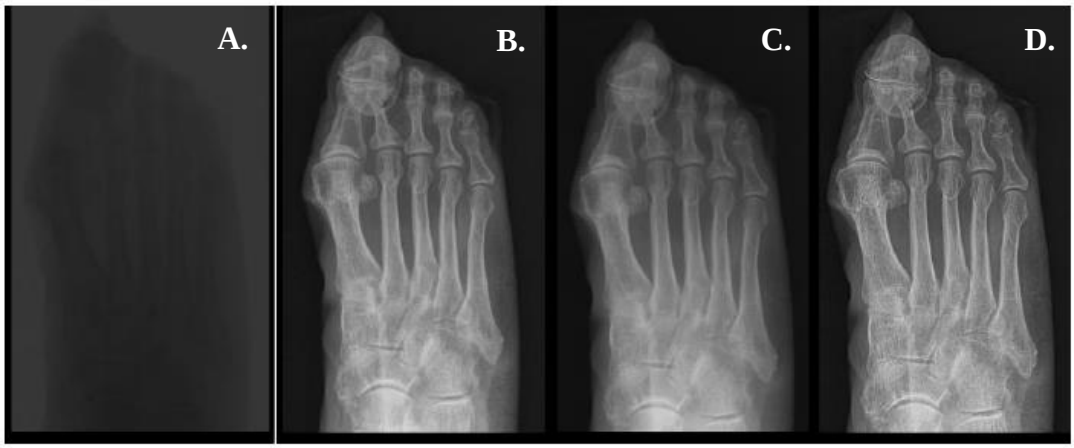

Figure 2.4 Digitally processing on image appearance: Raw data without any processing (A), Contrast enhancement (B), Contrast reduction (C) and Edge enhancement (D)(2).

2.1.4 Factors affecting image quality

A number of factors affecting the quality of the image in digital radiography are contrast, spatial resolution (detail), and noise. They are the primary factors and play a major role in CR and DR.

2.1.4.1 Contrast

Contrast (radiographic contrast) is proportional to the magnitude of the signal difference between the structure of interest and its surroundings in the displayed image, which is expressed in terms of the relative brightness difference between the corresponding areas in a digital image displayed on a monitor. Radiographic contrast is influenced by subject contrast and receptor sensitivity. However, in digital imaging, contrast in the displayed image can also be altered by the adjustment of display parameters independent of the acquisition parameters. Subject contrast is proportional to the relative difference in x-ray exposure on the exit side of the patient and is the result of the attenuating properties of the tissues under study. Attenuation is strongly dependent on the x-ray energy spectrum and is determined by the target material, kilovoltage, and total beam filtration. Subject contrast is further reduced by the presence of scatter. Receptor sensitivity is defined as the amount by which the output (analog-to-digital unit value for CR and DR) changes per unit change in exposure to the receptor (8).

The quantity of contrast shows how well two adjacent objects can be distinguished as separate entities and the differences in the attenuation properties of objects. The figure 2.5 illustrates the concept of contrast.

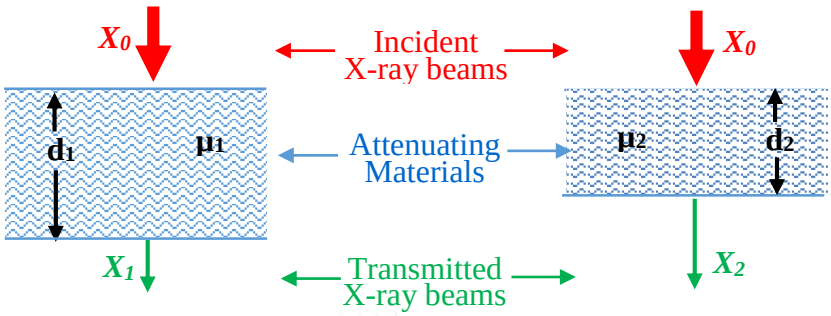

Figure 2.5 A schematic diagram illustrating the concept of contrast.

Any perception of contrast will be due to the difference in the transmitted intensities through the attenuating materials. The transmitted intensities X_1 and X_2 are related to contrast through the relationship:

$$\boldsymbol{Contrast = log_{10}\frac{X_1}{X_2}} \qquad \textbf{or}$$

$$\boldsymbol{Contrast = 0.43(\mu_1 X_1 - \mu_2 X_2)}$$

As beam energy increases, the Compton Effect becomes predominant, leading to increased scattered radiation which will ultimately reduce the contrast. In simple terms contrast is a measure of the difference between densities on an exposed detector.

For DR, image processing is used to determine display contrast by establishing the relationship between raw pixel values and gray-scale levels. This produces the final for-presentation image for interpretation either on hard-copy film or softcopy displays.

2.1.4.2 Spatial Resolution

Spatial resolution is the ability of an imaging system to allow two adjacent structures to be visualized as being separate, or the distinctness of an edge in the image (i.e., sharpness). Spatial resolution losses occur because of blurring caused by geometric factors (e.g., the size of the x-ray tube focal spot, light diffusion in the receptor), the effective aperture size, and motion of the patient relative to the x-ray source and image receptor.

The measurement of spatial resolution is performed by subjective or objective methods. Subjective measurement is achieved with a bar pattern of alternating radio-opaque bars and radiolucent spaces of equal width, imaged to determine the limiting resolution in line pairs per unit of distance, usually expressed in units of line pairs per millimeter. Intrinsic detector resolution measurements are performed by fixing the bar pattern to the receptor surface to eliminate focal spot blurring. System resolution (including the effects of the focal spot blur) uses a bar pattern placed at a clinically relevant distance above the receptor. For digital systems, the resolution may be different in the row and column directions, often requiring separate evaluations. The limiting resolution is the frequency at which the bars and spaces can no longer be visualized. Objective measurements by the MTF are obtained by measuring the transfer of signal amplitude (contrast) of sinusoidal patterns (of various frequencies) from incident x-rays to the output. The system MTF is determined by the product of the individual MTF components along the signal chain. The system MTF can be measured by imaging a test object containing a narrow slit or a sharp edge(8).

Spatial resolution in DR systems depends primarily on two factors. The first factor for indirect systems is the spread of light photons in the x-ray-to-light conversion process. To minimize visible photon spread, several manufacturers of indirect DR systems use structured converters, in which the converter material (usually cesium iodide) is formed into narrow, parallel columnar structures, oriented so that the x-ray photons are incident along the long dimension of the columns. The advantage of this structure is that the majority of the light exiting the converter onto the TFT array has been internally reflected along the length of the columns. The internal reflection process thus confines the light photons to a region close to the actual location of the x-ray absorption. This approach permits improved absorption efficiency through thicker

absorbers (longer columns) without as much spatial resolution degradation as seen in unstructured converters constructed using the same thickness. Direct-conversion DR systems do not suffer from this effect, because the spread of the electrons within the photoconductor material as they are accelerated toward the TFT array is minimal(8).

The second factor affecting spatial resolution is the size of photoconductor material. Because all x-rays absorbed within a single detector during an exposure contribute to a single quantity, there is no way to distinguish different absorption locations within a single detector. Therefore, structures in the patient smaller than the detector size are smeared out, and their contrast is reduced (this is known as the partial volume effect). Such structures may thus be undetectable unless they are inherently high contrast objects(8).

2.1.4.3 Noise

In radiography, noise can be defined as any fluctuations in an image that do not correspond to variations in the x-ray attenuation of the object being imaged. Image noise is typically measured by illuminating the receptor with a uniform x-ray fluence, then measuring the variance (the square of the standard deviation) in selected regions of the resulting image. A more informative measure of noise can be obtained by estimating the noise power spectrum (NPS), which characterizes the spatial frequency dependence of the noise. Knowledge of the frequency response of noise in an imaging system is important because there are a number of additional noise sources in digital radiography, such as aliasing and electronic noise that are not present in conventional (Film-Screen) systems(9).

The NPS can be thought of as the variance of the image intensity divided among the various frequency components of the image or as the variance of a given spatial frequency component in an ensemble of measurements of that spatial frequency. NPS is related to MTF and two dimensional DQE through the relationship.

$$DQE_{(u,v)} = \frac{d^2\, MTF^2_{(u,v)}}{qNPS_{(u,v)}}$$

Where d is the average pixel value in an image

$MTF_{(u,v)}$ is the two-dimensional system modulation transfer function

q is the average density of X-ray quanta incident on the system while the image is being acquired

NPS is the noise power spectrum which is a measure of the radiographic mottle.

DQE is the detector quantum efficiency

The level of noise depends on the amount of receptor exposure used to produce an image. With digital radiography it can be adjusted over a rather wide range because of the wide dynamic range of the typical digital receptor.

2.1.4.4 Image Processing

For digital imaging, image processing (which is often proprietary to the device manufacturer and not under the control of the radiologist) is used to determine display contrast by establishing the relationship between raw pixel values and grayscale levels(10).

2.1.4.4.1 Pre-processing

The image receptor on most digital radiography systems stores an electronic charge that is monotonically related to the amount of radiation energy absorbed. At this stage, the signal (charge) is a linear function of the incident radiation exposure. Preamplifiers and an analog-to-digital converter transform the charge from each detector element to an integer representing the raw data image value. Several corrections are applied to the raw image values to obtain values suitable for image processing. These corrections include interpolating bad pixels and to adjusting for non-uniformity(10).

2.1.4.4.2 For-Processing Images

Most DR systems transform the preprocessed value to a value proportional to the logarithm of the input exposure. Logarithmic signals have the property that a fractional change in signal, due to the contrast of adjacent structures, produces a fixed change in the raw image value independent of subject penetration and input exposure. These values are the *For-Processing* images values and may be stored in DICOM image objects. The AAPM further recommends specific units for normalized For-Processing image values(10).

2.1.4.4.3 DR Image Processing Operations

Image processing operations are performed on For Processing images to obtain For-Presentation images with values suitable for display on a workstation monitor. All suppliers of DR equipment provide image processing software that can restore the sharpness of edges, enhance detail contrast for images with a wide range of input exposures, and reduce noise. When properly implemented, image processing can restore the sharpness of edges without introducing artifacts. Detail contrast can be enhanced by multi-frequency processing that equalizes image brightness over broad areas by operating on low spatial frequencies. Most recently, methods have been introduced to reduce high frequency image noise without adversely effecting image resolution. In general, the image processing from different systems can be adjusted to give similar presentation appearance for images of the same body part, as the desired appearance may be different in different facilities. The parameters used to process images need to be specifically determined for all body parts and views that will be encountered. In the past, this required significant effort by the user to establish the desired appearance for all views. Currently, most systems make these adjustments internally, with the user determining the generic characteristics of the presented image. For example, users may differ with respect to the amount of detail contrast enhancement that is desired(10).

2.1.4.4.4 DR Image Grayscale

As a part of the operations that transform *For-Processing* images to *For-Presentation* images, the image values in the anatomical regions of interest referred to as the values of interest (VOI), are identified and used to compute a LUT used to display the *For-Presentation* values. Earlier systems applied the VOI-LUT in the DR systems and sent these image values within the DICOM object. It is preferable that the VOI-LUT be sent and that the image display software transform the values at the workstation. This allows the user at the workstation to make further adjustment in the grayscale of the image. The VOI are also used to calculate the exposure index and associated deviation index that are used as indicators of proper radiographic technique. The edges of the collimated regions of the image should be recognized by the system and the regions outside of the collimators masked to prevent presentation of large bright

regions to the radiologist, and to ensure accurate computation of the exposure indicator. It is preferable that this mask be encoded in the DICOM image as an overlay so that if needed it can be removed to see information that might be near the collimated edge, such as a marker(10).

2.1.5 Factors affecting radiation dose

2.1.5.1 Beam energy and filtration

Beam energy primarily depends on the peak kilovoltage (kVp) selected and the amount of filtration in the beam. If all other variables are held constant, radiation dose will change as the square of the change in peak kilovoltage. The selection of higher peak kilovoltage increases the average energy of the x-rays and therefore beams penetrability. As the beam becomes more penetrating, more x-rays will reach the image receptor during the same period of time. In practice, this may allow for use of a lower tube current or a shorter exposure, thus reducing the dose to the patient.

Diagnostic radiography units are required by regulations to contain a total filtration of at least 2.5 mm of aluminum equivalent if they are operated at tube potentials above kVp 70. This filtration preferentially absorbs the low-energy x-rays in the beam(11).

2.1.5.2 Collimation

During any radiographic procedure, the area of the patient exposed to the x-ray beam should be limited to the area of clinical interest. Tissues inside the primary beam receive doses that are orders of magnitude higher than doses received by tissues outside the primary beam. By using collimation to expose only the area of clinical interest, one can substantially reduce unnecessary patient exposure (11).

2.1.5.3 Grids

Grids were introduced into radiography to reduce the amount of scattered radiation that reaches the image receptor, resulting in images with much improved contrast and increased patient dose. A grid also absorbs a portion of the primary x-rays that would have contributed to exposing the image receptor and the only way to achieve the degree of exposure required to produce the image is to increase the amount of

radiation incident on the grid and therefore the patient. A grid removes a much larger fraction of scattered x-rays than primary x-ray, and the doses are typically increased from two to five times those encountered without the use of a grid. This proportion is commonly referred to as the Bucky factor and represents the ratio of the dose with a grid to the dose without a grid. The higher-quality images achieved with grid, however, may result in fewer retakes and more accurate diagnoses(1).

2.1.5.4 Patient size

As the thickness of the area being imaged increases, the amount of radiation incident on the patient increases because adequate x-ray penetration is needed to create an acceptable image. Technique charts that display suggested radiographic technique factors for various examinations and patient thicknesses placed near the operator's console may be helpful(11).

2.1.6 Image quality in Chest radiography

Image quality in chest radiography is usually considered in terms of the portrayal of normal anatomy or the depiction of potential pathology. Radiographic display of normal anatomy provides examples of the compromises that arise when image quality is considered. As one example, technical factors that might improve the visibility of unobscured lung may tend to diminish the visibility of lung projecting behind the heart or mediastinum. Consideration of such compromises often dominates careful investigations of image quality for the examination. Although thoracic anatomy is predictable in a given patient, potential abnormal findings are much less and it is not advisable to discuss image quality without reference to a target abnormality of interest. Lesions of clinical importance in chest radiography that might typically escape detection due to poor image quality include small, faint, opacities resulting from an early neoplasm or faint linear opacities caused by early interstitial disease. Technical approaches that might increase the likelihood that one type of target is detected can often decrease the likelihood of the detection of another. Discussions of image quality in chest radiography are most frequently framed in the context of detection of early neoplastic manifestations(12).

The concept of image contrast, image sharpness and image noise are the mainstays in the quantification of image quality in medical radiographic science(12).

2.1.7 Observer performance methods based on visibility of anatomical structures

2.1.7.1 Visual grading analysis

In visual grading analysis (VGA), the appearance of the whole image or part of an image is evaluated visually. A special case of VGA is to compare the visibility of defined structures with the same structures in a reference images(13).

The VGA approach to image assessment the image or a feature of the image is given a relative score, which reflects how well that image or feature can be visualized. The relative approach involves a comparison between the clinical test images and a reference image. Subsequently the observer gives a score or rates the clinical images with respect to the reference image. Results of the VGA study are then used to calculate the visual grading analysis score, which is defined as the mean of all the ratings when the numerical representations of the scale steps are used. The normalized visual grading analysis score (VGAS) can be calculated from(9)

$$VGAS = \frac{\sum_{i=1}^{I}\sum_{s=1}^{S}\sum_{o=1}^{O} G_{i,s,o}}{I * S * O}$$

Where G is the relative ratings of the image are summed over a number of observer (o), images (i) and structure (s).

I is the total number of images per technique

S is the total number of structures

O is the total number of observers

The VGA results are dependent on the reference image. VGA is very much a subjective test thus it can be improved by having multiple observers and averaging their scores(9).

2.1.7.2 Image criteria score

A special case of visual grading analysis is the use of image criteria. The criteria state various levels of visibility of defined structures (e.g. "visually sharp reproduction of the pedicles"). The task of the observer is to decide whether the criterion is fulfilled or not in an image. With this method an absolute level of image quality can be determined from what is stated in the criterion, with the frame of reference of the observer, provided that the observer's decision threshold is constant. The CEC has presented a list of image criteria in the European guidelines on Quality Criteria for Diagnostic Radiographic Images (European Commission, 1996)(13).

2.2 Related literature

Coblentz LC et al (14) proposed the guideline for mobile chest radiography. For the cooperative patients, erect radiographs at 180 cm target-film distance are preferred. For the uncooperative patients, a semi-erect or supine radiograph is necessary, and a 125 cm target-film distance is acceptable. Radiographic exposure should be made during peak inspiration. The kilo-voltage should be between 80 and 90 in order to optimize penetration and minimize the effects of scattered radiation. Grids should be used whenever possible and higher kilo-voltage ranges of 100-120 are employed. To minimize patient motion, mobile equipment should have adequate capacity to make a radiographic exposure in less than 0.1 seconds. Exposure parameters such as mAs, kVp, distance and patient position should be recorded as they may be helpful in future radiographs taken at the bedside.

Sun Z et al (15) studied the performance of three computed radiography and three direct radiography systems with regard to the image noise and entrance skin dose based on a chest phantom. Images were obtained with kVp of 100, 110, and 120 and mA settings of 1, 2, 4, 8, and 10. Quantitative measurements of image quality were conducted at seven regions of interest to determine the relationship between image noise, imaging parameters, and different digital systems. The selected regions of interest (ROIs) at middle right 4^{th} rib (ROI 1), area to the left of the right 4^{th} rib soft tissue reading (ROI 2), interspace between third rib and fourth rib (ROI 3), middle of the spine (ROI 4), heart beside the step wedge (ROI 5), area below the diaphragm (ROI

6) and left side of abdomen (ROI 7). Image noise was defined as the standard deviation (SD) of the pixel value within the region of interest. Significant differences of image noise were found in these digital chest radiography systems *(*P<0.0001). Standard deviation was significantly different when the mAs was changed (P<0.0001), but it was independent of the kVp values (P=0.08–0.85). Up to 44% of radiation dose could be saved when kVp was reduced from 120 to 100 without compromising image quality.

Anderson DW et al (16) compared image quality before and after introducing grid use routinely to the mobile x-ray. This was studied in the intensive care unit (ICU) setting, comparing images obtained over a 2 week period prior to and after the introduction of the change in technique. They introduced a 6:1 grid ratio with appropriate changes in exposure factors. No other alterations were made. The images were graded for diagnostic quality using a five point grading system as follows: Grade 1 was not of diagnostic quality, Grade 2 was poor or barely adequate diagnostic quality, Grade 3 was fair or acceptable diagnostic quality, Grade 4 was good or above average diagnostic quality and Grade 5 was excellent diagnostic quality. The initial image set performed before grid technique (total 133 patients) produced the following results: Grade 1: 24/133, Grade 2: 55/133, Grade 3: 40/133, Grade 4: 13/133 and Grade 5: 1/133. The second image set, performed following the introduction of grid technique (total 196 patients) produced the following results: Grade 1: 2/196, Grade 2: 30/196, Grade 3: 104/196, Grade 4: 48/196 and Grade 5: 12/196. They found that a reduction in the proportion of images were of non-diagnostic or barely diagnostic quality. Non-diagnostic examinations were reduced from 18% to 1%. Introducing grids to mobile x-ray resulted in improvement in image diagnostic quality, largely by reducing the proportion of poor and unacceptable quality images.

Schaefer-Prokop RC et al (17) presented the relationship between dose and image quality quantitatively and qualitatively. The spectrum reaches from objective measurements of physical characteristics, such as modulation-transfer function (MTF), detective quantum efficiency (DQE) or contrast-noise ratio (CNR) over contrast-detail studies, anthropomorphic phantom studies to clinical studies. Studies differ in how much a radiologist's perception and abilities are involved and how well they represent the clinical situation.

A review of the literature concluded that the primary factors affecting image quality in digital radiography consists of contrast, spatial resolution and noise. The factors affecting radiation dose are beam energy, kVp, collimation, anti-scatter (grid) and patient size. Image quality in chest radiography considered in terms of the portrayal of normal anatomy or depiction of potential pathology.

The purpose of this research is to study the exposure parameters for the bedside digital chest radiography based on image quality and patient dose.

CHAPTER 3
RESEARCH METHODOLOGY

3.1 Research design

This is an observational cross-sectional descriptive study.

3.2 Research design model

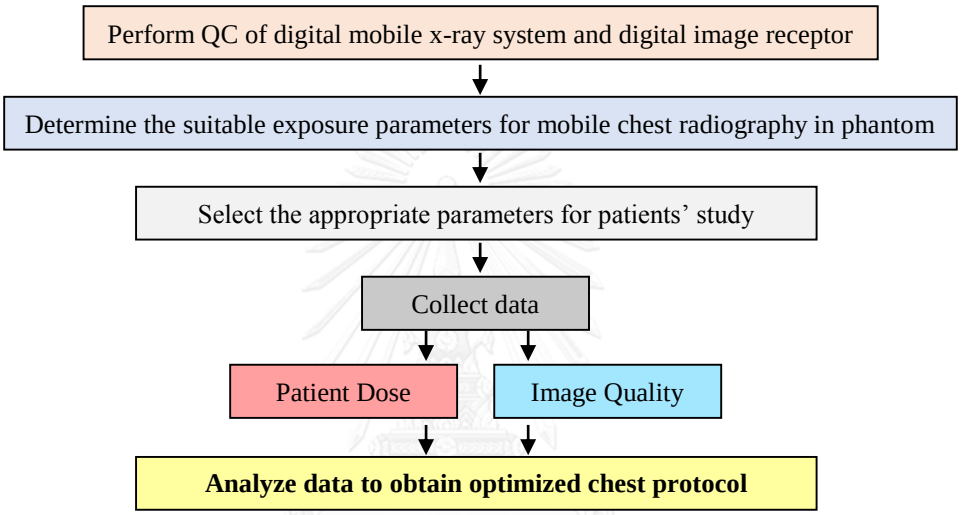

3.3 Conceptual framework

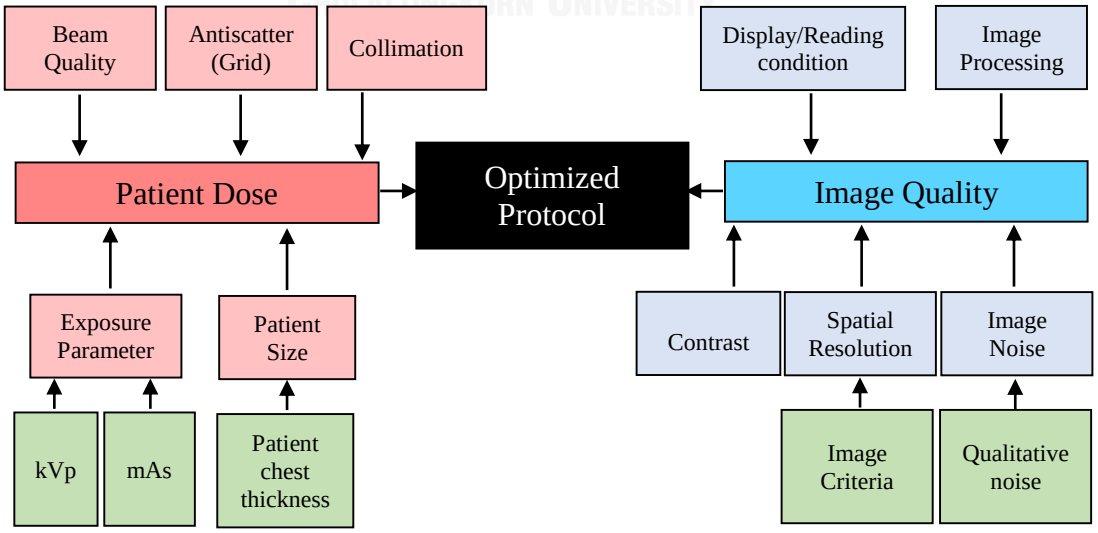

3.4 Research question

What is the exposure parameter for chest radiography using digital mobile x-ray system to optimize radiation dose and image quality?

3.5 Research objective

To optimize the radiation dose and image quality for chest radiograph using digital mobile x-ray system at King Chulalongkorn Memorial Hospital.

3.6 Materials

3.6.1 Digital mobile x-ray system

Digital mobile x-ray system manufacturer GE, model Optima XR220amx S/N. 1031650WK3 with digital image receptor S/N.UA45948-6 at Department of Radiology, King Chulalongkorn Memorial Hospital as shown in figure 3.1.

Figure 3.1 Digital mobile x-ray GE Optima XR220amx and Digital image receptor.

3.6.2 Ionization chamber dosimeter

The ACCU-PRO ionization chamber dosimeter manufacturer Radcal Corporation model AGDM S/N.40-0277 measured the radiation for the calculation of the scattered radiation (figure 3.2).

Figure 3.2 Ionization Chamber dosimeter manufacturer Radcal model AGDM.

3.6.3 Solid state dosimeter

Solid state dosimeter manufacturer UNFORS RaySafe model Xi S/N.167273 and Detector S/N. 166743 was used to calibrate the Digital mobile x-ray system and measure the radiation dose from phantom study. The dosimeter measured kVp, dose, dose rate, pulse, pulse rate, time, HVL, total filtration and waveforms simultaneously (figure 3.3).

Figure 3.3 Solid state dosimeter manufacturer UNFORS RaySafe model Xi.

Table 3.1 Specifications of UNFORS RaySafe model Xi

Model Xi	
Size	12 x 22 x 117 mm
DOSE	
Range	10 nGy – 9999 Gy
Trig level	100 nGy/s
Uncertainty	5 % (40 – 150 kVp, HVL: 1.5 – 14 mm Al (1), Active Compensation)
DOSE RATE	
Range	10 nGy/s – 1 mGy/s
Min. peak trig level	100 nGy/s
Uncertainty	5 % (40 – 150 kVp, HVL: 1.5 – 14 mm Al (1), Active Compensation)
kV/kVp	
Range	35 – 160 kV/kVp (for up to 0.5 mm Cu or equivalent)
	60 – 130 kV/kVp (for 0.5 - 1 mm Cu or equivalent)
Uncertainty	2 % (for up to 0.5 mm Cu or equivalent, Active Compensation)
	3 % (for up to 0.5 – 1 mm Cu or equivalent, Active Compensation)
EXPOSURE RATE	
Range	1 ms – 999 ms
Uncertainty	0.5 % or 0.2 ms
HVL	
Range	1.0 – 14.0 mm Al
Uncertainty	10 % (at signal level above 1/1000 of max dose rate for selected sensor)
TOTAL	
FILTRATION	
Range	1.5 – 35 mm Al (60 – 120 kV)
Uncertainty	10 % or ± 0.3 mm Al

3.6.4 Multipurpose chest phantom

Chest phantom manufacturer Kyoto Kagaku Co.Ltd. model N1 LUNGMAN (male chest torso) is designed and constructed commercially to simulate standard human chest as shown in figure 3.4. X-ray absorption rates relatively to those of human tissues.

Figure 3.4 Multipurpose chest phantom N1 LUNGMAN.

Table 3.2 Specifications of Multipurpose chest phantom N1 LUNGMAN

N1 LUNGMAN	
Main body:	Synthetic bones are embedded
Internal parts:	1. Mediastinum: Heart, Trachea
(separates into four parts)	2. Pulmonary vessels (right and left)
	3. Abdomen (diaphragm) block: no internal structure
	4. 15 Simulated tumors:
	• 3 varieties of Hounsfield number: approx. -800, -630, +100
	• 5 sizes for each type: diameters 3, 5, 8, 10, 12 mm
Material:	Soft tissue: polyurethane (gravity 1.06)
	Synthetic bones: epoxy resin
Phantom size:	43 x 40 x 48H cm, chest girth 94 cm
	Weight: approx. 18 kg
Packing size:	59 x 52 x 30 cm, 25 kg

3.6.5 The patients

The patients underwent mobile digital chest radiography at In-Patient Department of Radiology, King Chulalongkorn Memorial Hospital.

3.7 Methods

The study was carried out as in the following sequences

3.7.1 Perform Quality Control of digital mobile x-ray system

The quality control of digital mobile x-ray system was performed following the AAPM report No.74 (18). The quality control program consists of the test of performance of electromechanical components, image quality and radiation dose. The x-ray equipment and dosimeter set up for quality control procedures were shown in figure 3.5.

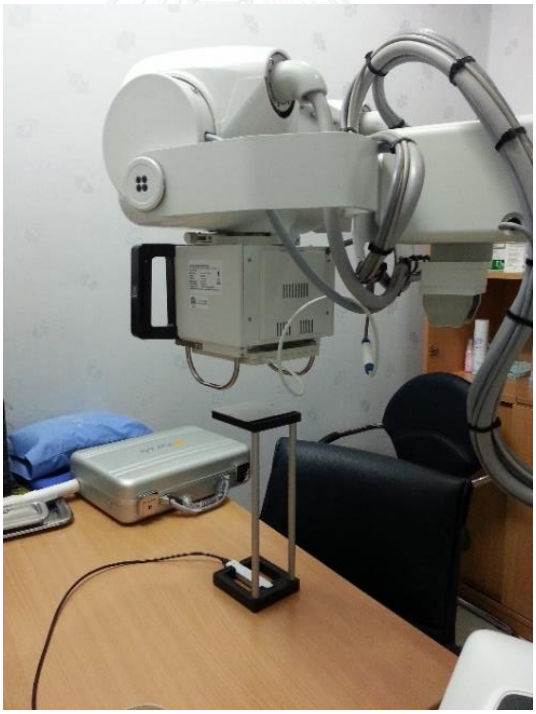

Figure 3.5 Set-up for quality control of x-ray beam quality.

3.7.2 Perform Quality Control of GE Digital image receptor

The quality control of digital image receptor was performed following the KCARE protocol for the QC of direct digital radiography system(19). The tests were intended to detect artefacts and test image quality and sensitivity. The tests were split into the following categories;

- Commissioning tests
- Annual QA tests.

3.7.3 Determine the backscatter factors

The backscatter factor from the LUNGMAN phantom was determined for varying exposure parameters of kVp 70-120 as following

3.7.3.1 Set up the digital mobile x-ray unit and ionization chamber dosimeter as followings, 77 cm of Source to Chamber Distance (SCD), 100 cm of Source to Detector Distance (SDD) and 41x41 cm of field size (Figure 3.6).

Figure 3.6 Set up for the incident air kerma, K_i measurement

3.7.3.2 Set kVp at 70, 80, 90, 100, 110 and 120 and mAs at 1.0, 2.5, and 5.0, expose the ionization chamber to determine K_i as in figure 3.6.

3.7.3.3 Set the LUNGMAN phantom under the ionization chamber to measure the entrance surface air kerma, K_e (Figure 3.7).

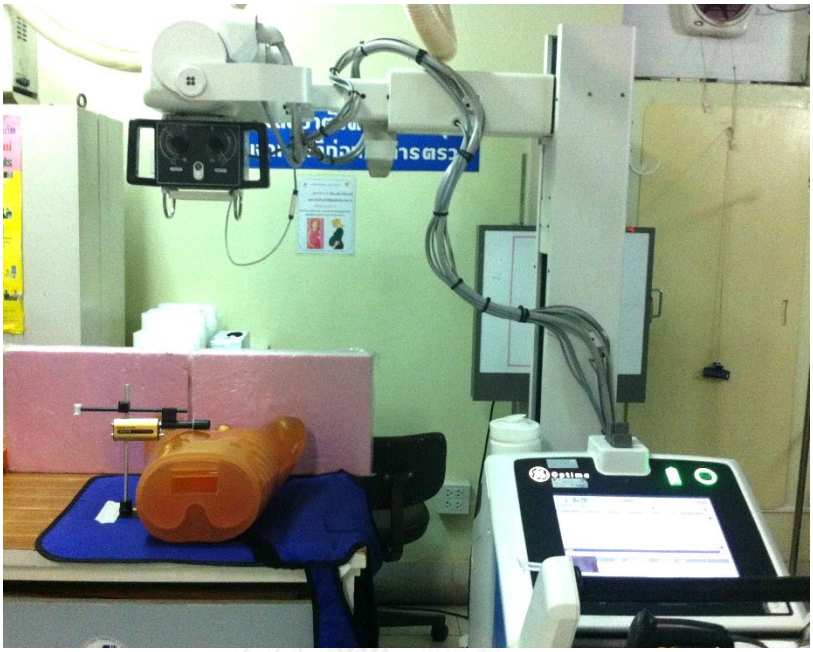

Figure 3.7 Set up for the entrance surface air kerma, K_e measurement

3.7.3.4 Set kVp at 70, 80, 90, 100, 110 and 120 and mAs at 1.0, 2.5, and 5.0, expose the ionization chamber to determine K_e as in figure 3.7.

3.7.3.5 Back Scatter Factor (BSF) can be calculated by the following equation.

$$\boldsymbol{BSF = \frac{Entrance\ surface\ air\ kerma}{incident\ air\ kerma}}$$

3.7.4 Calculate the ESAK for the phantom study

The ESAK for 23 cm thickness of LUNGMAN phantom was calculated for varying exposure parameters of kVp 70-120 and mAs 0.2-10.0 at FID 100 cm. The ESAK was calculated by the equations:

$$\boldsymbol{Y(d) = \frac{K(d)}{P_{It}}}$$

$$\boldsymbol{K_i = Y(d).P_{It}.\left(\frac{d}{d_{FTD} - t_P}\right)^2}$$

$$\boldsymbol{ESAK = K_i.BSF}$$

Where: $Y(d)$ = X-ray tube output

$K(d)$ = Air kerma

P_{It} = Tube loading

K_i = Incident air kerma

d = Focus to chamber distance

d_{FTD} = Focus to table distance

t_P = Patient thickness

ESAK = Entrance Surface Air Kerma

BSF = Back Scatter Factor

The unit of entrance surface air kerma is mGy

3.7.5 Phantom study

The phantom study was performed using the exposure parameter that the ESAK was less than 0.4 mGy (IAEA DRL of Chest radiography). The set up for x-ray equipment and LUNGMAN phantom was shown in figure 3.8

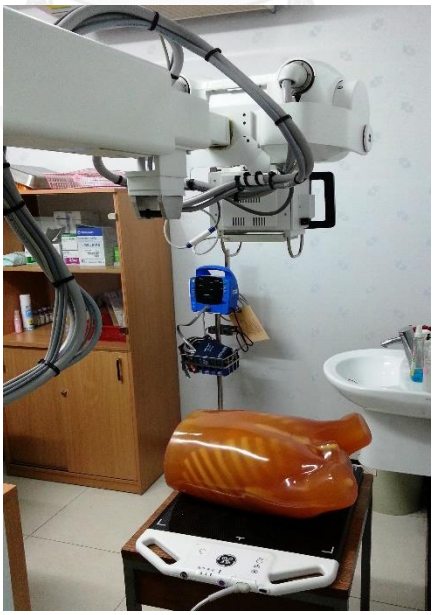

Figure 3.8 Set up for the phantom study.

3.7.6 Optimize the radiation dose and image quality from phantom to obtain the appropriate protocols for patients.

The appropriate protocol is based on the image quality score and the radiation dose. The image quality of the phantom radiographs was evaluated by three observers in term of;

3.7.6.1 Image criteria score based on the Commission of the European Communities (CEC) criteria as shown in table 3.3.

Table 3.3 Score image criteria based on the Commission of the European Communities

Item	Image Criteria	Score*
1	Visually sharp reproduction of the vascular pattern in the whole lung, particularly the peripheral vessels	
2	Visually sharp reproduction of the trachea and proximal	
3	Visually sharp reproduction of the borders of the heart and	
4	Visually sharp reproduction of the diaphragm and lateral	
5	Visualization of the retrocardiac lung and the mediastinum	
6	Visualization of the spine through the heart shadow	

* Rate image score: 0, 0.5 and 1 where 0 = not fulfilled, 0.5 = partly fulfilled, 1 = fulfilled

3.7.6.2 Qualitative noise score: relative rating score as

- Score 3 = Free of noise
- Score 2 = Scarce noise
- Score 1 = Significant noise
- Score 0 = Obvious noise

3.7.7 Collect the data of routine exposure protocol

Before the patient study, the patient exposed by digital mobile x-ray system of routine exposure protocol was collected. Record the patient's information such as the thickness of chest, exposure parameter (kVp and mAs).

3.7.8 Collect the data of patient study

The appropriate protocol from phantom study was used for the patient who underwent mobile chest radiography. Record the patient's information such as the thickness of chest, exposure parameter, field size and focus to image receptor distance (FID).

3.7.9 Determine patient dose and image quality assessment

3.7.9.1 Patient dose calculation

Calculation the patient dose by using the equation in 3.7.4

3.7.9.2 Image quality assessment

The image quality of the chest radiographs was evaluated by three observers using the same method of phantom study.

3.7.10 Define the acceptable level of chest radiographs for clinical diagnosis.

3.7.11 Analyze the image quality and correlate with the patient dose.

3.7.12 Obtain the optimal protocol for mobile chest radiography in patient.

3.7.13 Compare the average patient dose from patient study to routine protocol.

3.8 Sample size determination

3.8.1 Target population

The patients were requested for portable chest AP radiographic projection using digital mobile x-ray at King Chulalongkorn Memorial Hospital.

Inclusion criteria:

- Patients' chest thickness: 15 to 23 cm.

Exclusion criteria:

- Patient's chest thickness: Less than 15 cm or more than 23 cm.
- Poor image quality or motion unsharpness.

3.8.2 Sample population

The sample size was determined using formula as following

$$N = \frac{(Z_{\alpha/2})^2 \cdot \sigma^2}{d^2}$$

$$N = \frac{(1.96)^2 \cdot (0.25)^2}{(0.1)^2}$$

N = 24.01 50 cases will be collected

Where: N = Sample size

$Z_{\alpha/2}$ = 95% Confidence Interval (1.96)

σ^2 = Variance of data (0.25)

d = Acceptable error (0.1)

3.9 Statistical analysis

3.9.1 Descriptive statistics: mean, standard deviation (SD), minimum and maximum of radiation dose, percentage of the score of image criteria and qualitative noise were determined using Microsoft excel.

3.9.2 Weighted Kappa for inter-observer reliability was used to evaluate the image criteria and qualitative noise score analysis.

3.10 Outcomes

3.10.1 The optimal protocol for mobile chest radiography.

3.10.2 The patient radiation dose calculated from patient thickness, kVp and mAs.

3.10.3 The image quality scored by three observers on

3.10.3.1 Image criteria score

3.10.3.2 Qualitative noise score

3.11 Data Collection

3.11.1 Patient dose: thickness of chest, exposure parameter (kVp, mAs), and FID.

3.11.2 Image quality: image criteria score and qualitative noise score.

3.12 Data Presentation

The table, bar diagram and scatter chart were presented in terms of patient dose, image criteria score and qualitative noise score.

3.13 Expected Benefit

The optimal protocol for mobile chest radiography will be obtained. These would be beneficial to the patients who receive low dose and accepted image quality, referred physicians for follow up clinical disease and radiographers who apply for the optimal protocols.

3.14 Limitation

There are no image criterion for chest radiography in AP supine position. Thus, the image criteria from chest radiography in PA upright position based on the Commission of the European Communities (CEC) criteria to evaluate the image quality had been applied.

The LUNGMAN phantom has only two sizes of 23 cm and 29 cm thickness (with build-up layer).This study used only a thickness of 23 cm, which is close to Thai patients.

3.15 Ethical consideration

The patient dose in this study will be directly evaluated in patient at In-Patient Department (IPD) of King Chulalongkorn Memorial Hospital. The research proposal has been approved by the Ethic Committee of Faculty of Medicine, Chulalongkorn University.

CHAPTER 4
RESULTS

4.1 Quality Control of digital mobile x-ray system

The quality control of digital mobile x-ray system was performed following the AAPM report No.74(18). The results were within acceptable range of the AAPM protocol. The detail of quality control and the performance test is shown in appendix A.

4.2 Quality Control of digital image receptor

The quality control of digital image receptor was performed following the KCARE protocol(19). The results were within acceptable range of the KCARE protocol. The detail of quality control is shown with the summarized report of digital image receptor as in appendix B.

4.3 The backscatter factors

The BSF was determined by set kVp at 70, 80, 90, 100, 110, 120 and mAs at 1.0, 2.5, 5.0. The results of backscatter factors (BSF) were shown as in table 4.1.

Table 4.1 The results of backscatter factor

Parameter		**Dosimeter reading (mGy)**		**BSF**	**Average**
kVp	**mAs**	K_i	K_e		
70	1.0	0.052	0.071	1.353	**1.353**
	2.5	0.131	0.177	1.353	
	5.0	0.270	0.366	1.353	
80	1.0	0.072	0.098	1.371	**1.370**
	2.5	0.184	0.252	1.370	
	5.0	0.363	0.497	1.370	
90	1.0	0.094	0.130	1.383	**1.382**
	2.5	0.238	0.330	1.382	
	5.0	0.466	0.644	1.382	
100	1.0	0.117	0.162	1.388	**1.388**
	2.5	0.291	0.404	1.387	
	5.0	0.580	0.805	1.388	

Table 4.1 The results of backscatter factor (Continued)

Parameter		Dosimeter reading (mGy)		BSF	Average
kVp	**mAs**	K_i	K_e		
110	1.0	0.145	0.202	1.391	**1.391**
	2.5	0.350	0.487	1.391	
	5.0	0.700	0.973	1.391	
120	1.0	0.164	0.229	1.394	**1.393**
	2.5	0.408	0.568	1.392	
	5.0	0.830	1.156	1.393	

4.4 ESAK for the phantom study

The ESAK for 23 cm thickness of phantom was calculated for varying exposure parameters of kVp 70, 80, 90, 100, 110 and120, mAs 0.2, 0.25, 0.32, 0.4, 0.5, 0.63, 1.0, 1.6, 2.0, 2.5, 3.2, 4.0, 5.0, 6.3, 8.0 and 10.0, at FID 100 cm using data from quality control of digital mobile x-ray system as shown in table 4.2. 96 ESAK were calculated based on the exposure parameters used for this study and ranged from 0.014 to 2.252 mGy as shown in figure 4.1.

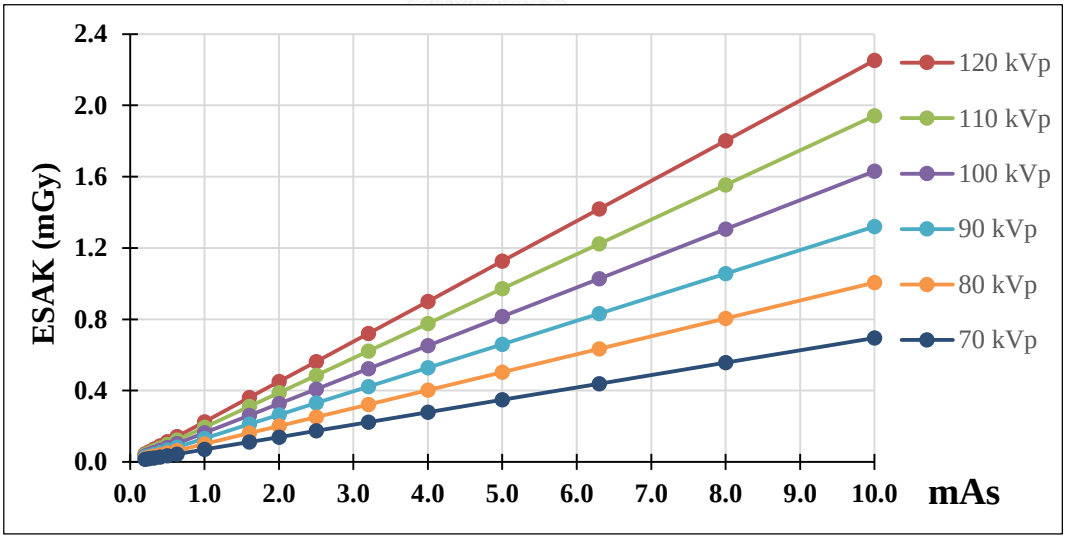

Figure 4.1 Relation of calculated ESAK and the exposure parameters

Table 4.2 The calculated ESAK from the phantom study.

Selected kVp	Tube loading: P_{It} or mAs	Tube output: Y(d) (mGy/mAs)	K_i (mGy)	BSF	ESAK (mGy)
70	**0.2**	0.07	0.010	1.353	**0.014**
70	**0.25**	0.07	0.013	1.353	**0.017**
70	**0.32**	0.07	0.016	1.353	**0.022**
70	**0.4**	0.07	0.021	1.353	**0.028**
70	**0.5**	0.07	0.026	1.353	**0.035**
70	**0.63**	0.07	0.032	1.353	**0.044**
70	**1.0**	0.07	0.051	1.353	**0.070**
70	**1.6**	0.07	0.082	1.353	**0.111**
70	**2.0**	0.07	0.103	1.353	**0.139**
70	**2.5**	0.07	0.129	1.353	**0.174**
70	**3.2**	0.07	0.165	1.353	**0.223**
70	**4.0**	0.07	0.206	1.353	**0.278**
70	**5.0**	0.07	0.257	1.353	**0.348**
70	**6.3**	0.07	0.324	1.353	**0.438**
70	**8.0**	0.07	0.411	1.353	**0.557**
70	**10.0**	0.07	0.514	1.353	**0.696**
80	**0.2**	0.10	0.015	1.370	**0.020**
80	**0.25**	0.10	0.018	1.370	**0.025**
80	**0.32**	0.10	0.024	1.370	**0.032**
80	**0.4**	0.10	0.029	1.370	**0.040**
80	**0.5**	0.10	0.037	1.370	**0.050**
80	**0.63**	0.10	0.046	1.370	**0.063**
80	**1.0**	0.10	0.073	1.370	**0.101**
80	**1.6**	0.10	0.118	1.370	**0.161**
80	**2.0**	0.10	0.147	1.370	**0.201**
80	**2.5**	0.10	0.184	1.370	**0.252**
80	**3.2**	0.10	0.235	1.370	**0.322**
80	**4.0**	0.10	0.294	1.370	**0.403**
80	**5.0**	0.10	0.367	1.370	**0.503**
80	**6.3**	0.10	0.463	1.370	**0.634**
80	**8.0**	0.10	0.588	1.370	**0.805**
80	**10.0**	0.10	0.735	1.370	**1.007**

Table 4.2 The calculated ESAK from the phantom study (Continued)

Selected kVp	Tube loading: P_{It} or mAs	Tube output: Y(d) (mGy/mAs)	K_i (mGy)	BSF	ESAK (mGy)
90	**0.2**	0.13	0.019	1.382	**0.026**
90	**0.25**	0.13	0.024	1.382	**0.033**
90	**0.32**	0.13	0.031	1.382	**0.042**
90	**0.4**	0.13	0.038	1.382	**0.053**
90	**0.5**	0.13	0.048	1.382	**0.066**
90	**0.63**	0.13	0.060	1.382	**0.083**
90	**1.0**	0.13	0.096	1.382	**0.132**
90	**1.6**	0.13	0.153	1.382	**0.211**
90	**2.0**	0.13	0.191	1.382	**0.264**
90	**2.5**	0.13	0.239	1.382	**0.330**
90	**3.2**	0.13	0.306	1.382	**0.422**
90	**4.0**	0.13	0.382	1.382	**0.528**
90	**5.0**	0.13	0.478	1.382	**0.660**
90	**6.3**	0.13	0.602	1.382	**0.832**
90	**8.0**	0.13	0.764	1.382	**1.056**
90	**10.0**	0.13	0.955	1.382	**1.320**
100	**0.2**	0.16	0.024	1.388	**0.033**
100	**0.25**	0.16	0.029	1.388	**0.041**
100	**0.32**	0.16	0.038	1.388	**0.052**
100	**0.4**	0.16	0.047	1.388	**0.065**
100	**0.5**	0.16	0.059	1.388	**0.082**
100	**0.63**	0.16	0.074	1.388	**0.103**
100	**1.0**	0.16	0.118	1.388	**0.163**
100	**1.6**	0.16	0.188	1.388	**0.261**
100	**2.0**	0.16	0.235	1.388	**0.326**
100	**2.5**	0.16	0.294	1.388	**0.408**
100	**3.2**	0.16	0.376	1.388	**0.522**
100	**4.0**	0.16	0.470	1.388	**0.653**
100	**5.0**	0.16	0.588	1.388	**0.816**
100	**6.3**	0.16	0.741	1.388	**1.028**
100	**8.0**	0.16	0.940	1.388	**1.305**
100	**10.0**	0.16	1.176	1.388	**1.632**

Table 4.2 The calculated ESAK from the phantom study (Continued)

Selected kVp	Tube loading: P_{It} or mAs	Tube output: Y(d) (mGy/mAs)	K_i (mGy)	BSF	ESAK (mGy)
110	**0.2**	0.19	0.028	1.391	**0.039**
110	**0.25**	0.19	0.035	1.391	**0.049**
110	**0.32**	0.19	0.045	1.391	**0.062**
110	**0.4**	0.19	0.056	1.391	**0.078**
110	**0.5**	0.19	0.070	1.391	**0.097**
110	**0.63**	0.19	0.088	1.391	**0.122**
110	**1.0**	0.19	0.140	1.391	**0.194**
110	**1.6**	0.19	0.223	1.391	**0.311**
110	**2.0**	0.19	0.279	1.391	**0.388**
110	**2.5**	0.19	0.349	1.391	**0.485**
110	**3.2**	0.19	0.447	1.391	**0.621**
110	**4.0**	0.19	0.558	1.391	**0.777**
110	**5.0**	0.19	0.698	1.391	**0.971**
110	**6.3**	0.19	0.879	1.391	**1.223**
110	**8.0**	0.19	1.117	1.391	**1.553**
110	**10.0**	0.19	1.396	1.391	**1.942**
120	**0.2**	0.22	0.032	1.393	**0.045**
120	**0.25**	0.22	0.040	1.393	**0.056**
120	**0.32**	0.22	0.052	1.393	**0.072**
120	**0.4**	0.22	0.065	1.393	**0.090**
120	**0.5**	0.22	0.081	1.393	**0.113**
120	**0.63**	0.22	0.102	1.393	**0.142**
120	**1.0**	0.22	0.162	1.393	**0.225**
120	**1.6**	0.22	0.259	1.393	**0.360**
120	**2.0**	0.22	0.323	1.393	**0.450**
120	**2.5**	0.22	0.404	1.393	**0.563**
120	**3.2**	0.22	0.517	1.393	**0.720**
120	**4.0**	0.22	0.647	1.393	**0.901**
120	**5.0**	0.22	0.808	1.393	**1.126**
120	**6.3**	0.22	1.018	1.393	**1.418**
120	**8.0**	0.22	1.293	1.393	**1.801**
120	**10.0**	0.22	1.616	1.393	**2.252**

4.5 Phantom study

4.5.1 Radiation dose (ESAK)

The ESAK of phantom study was acquired by 60 exposure parameters listed in table 4.3.The calculated ESAK is less than 0.4 mGy, IAEA Dose Reference Level for chest radiography. The range of ESAK from 0.014 to 0.388 mGy are shown in figure 4.3. The results of ESAK were presented as in table 4.4.

Table 4.3 kVp and mAs used in phantom study

kVp	mAs
70	0.2, 0.25, 0.32, 0.4, 0.5, 0.63, 1.0, 1.6, 2.0, 2.5, 3.2, 4.0, 5.0
80	0.2, 0.25, 0.32, 0.4, 0.5, 0.63, 1.0, 1.6, 2.0, 2.5, 3.2
90	0.2, 0.25, 0.32, 0.4, 0.5, 0.63, 1.0, 1.6, 2.0, 2.5
100	0.2, 0.25, 0.32, 0.4, 0.5, 0.63, 1.0, 1.6, 2.0
110	0.2, 0.25, 0.32, 0.4, 0.5, 0.63, 1.0, 1.6, 2.0
120	0.2, 0.25, 0.32, 0.4, 0.5, 0.63, 1.0, 1.6

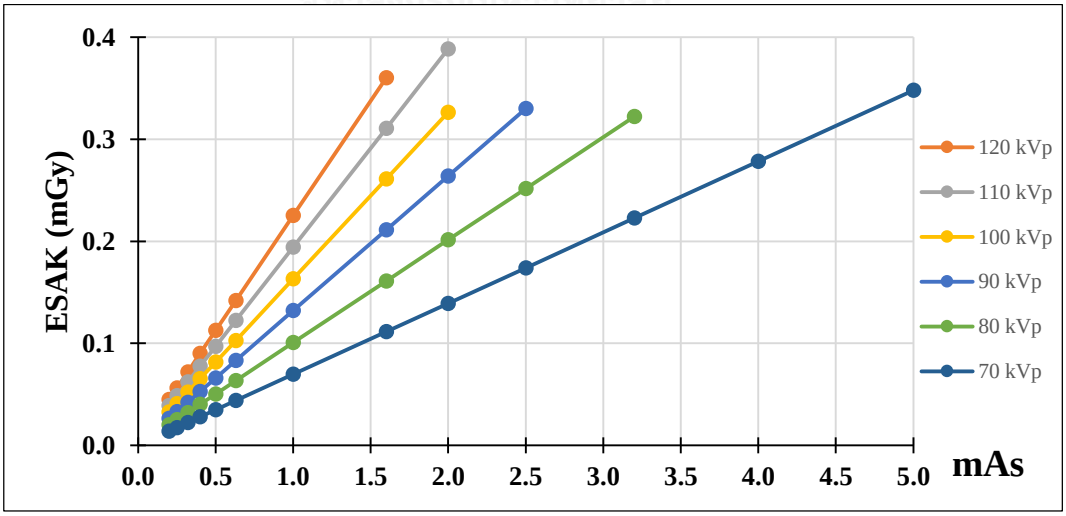

Figure 4.2 ESAK and exposure parameters used in phantom study.

4.5.2 Image quality of phantom study

The image quality was evaluated by three observers as shown in table 4.4.

Table 4.4 ESAK and image quality score of phantom study

Exposure parameter :kVp;mAs	ESAK (mGy)	1st Observer		2nd Observer		3rd Observer	
		Image criteria	Qualitative noise	Image criteria	Qualitative noise	Image criteria	Qualitative noise
70;0.2	0.014	2.5	0	2.5	0	2.5	0
70;0.25	0.017	2.5	0	2.0	0	2.5	0
70;0.32	0.022	3.5	0	3.0	1	3.0	1
70;0.4	0.028	4.0	1	4.5	1	4.5	1
70;0.5	0.035	5.0	1	5.0	1	5.5	1
70;0.63	0.044	5.5	1	5.5	1	5.5	1
70;1.0	0.070	4.5	1	4.0	1	4.0	1
70;1.6	0.111	5.0	2	5.0	2	5.0	2
70;2.0	0.139	5.0	2	5.0	2	5.0	2
70;2.5	0.174	5.5	2	5.5	2	5.0	2
70;3.2	0.223	5.0	2	5.0	2	5.0	2
70;4.0	0.278	5.0	3	5.5	2	5.0	3
70;5.0	0.348	5.5	3	5.5	3	5.0	3
80;0.2	0.020	4.5	1	4.5	1	4.5	1
80;0.25	0.025	5.0	1	5.0	1	5.0	1
80;0.32	0.032	5.0	1	5.5	1	5.5	1
80;0.4	0.040	5.5	1	5.5	1	5.5	1
80;0.5	0.050	5.0	1	5.0	1	5.5	1
80;0.63	0.063	5.0	1	5.0	1	5.0	1
80;1.0	0.101	5.0	2	5.0	2	5.0	1
80;1.6	0.161	5.0	2	5.0	2	5.0	2
80;2.0	0.201	5.0	2	5.0	2	5.0	2
80;2.5	0.252	5.5	2	5.0	2	5.5	2
80;3.2	0.322	5.5	3	5.5	3	5.5	3
90;0.2	0.026	5.0	1	5.0	1	5.5	1
90;0.25	0.033	5.5	1	5.5	1	5.5	1
90;0.32	0.042	5.5	1	5.5	1	5.5	1
90;0.4	0.053	5.5	1	5.5	1	5.5	1

Table 4.4 ESAK and image quality score of phantom study (Continued)

Exposure parameter :kVp;mAs	ESAK (mGy)	1st Observer		2nd Observer		3rd Observer	
		Image criteria	Qualitative noise	Image criteria	Qualitative noise	Image criteria	Qualitative noise
90;0.5	0.066	5.5	1	5.5	1	5.5	1
90;0.63	0.083	5.5	2	5.5	2	5.5	2
90;1.0	0.132	5.5	2	5.5	2	5.5	2
90;1.6	0.211	5.5	2	5.5	2	5.5	2
90;2.0	0.264	5.5	3	5.5	3	5.5	3
90;2.5	0.330	5.5	3	5.5	3	5.5	3
100;0.2	0.033	5.5	1	5.5	1	5.5	1
100;0.25	0.041	5.5	1	5.5	1	5.5	1
100;0.32	0.052	5.5	1	5.0	1	5.5	1
100;0.4	0.065	5.5	1	5.5	1	5.5	1
100;0.5	0.082	5.5	1	5.5	1	5.5	1
100;0.63	0.103	5.5	2	5.5	2	5.5	1
100;1.0	0.163	5.5	2	5.5	2	5.5	2
100;1.6	0.261	5.5	2	5.5	2	5.5	2
100;2.0	0.326	5.5	3	5.5	2	5.5	3
110;0.2	0.039	5.5	1	5.5	1	5.5	1
110;0.25	0.049	5.5	1	5.5	1	5.5	1
110;0.32	0.062	5.5	1	5.0	1	5.5	1
110;0.4	0.078	5.5	1	5.5	1	5.5	1
110;0.5	0.097	5.5	1	5.0	1	5.5	1
110;0.63	0.122	5.5	2	5.5	2	5.5	2
110;1.0	0.194	5.5	2	5.5	2	5.5	2
110;1.6	0.311	5.5	2	5.5	2	5.5	2
110;2.0	0.388	5.5	3	5.5	3	5.5	2
120;0.2	0.045	5.5	1	5.5	1	5.5	1
120;0.25	0.056	5.5	1	5.5	1	5.5	1
120;0.32	0.072	5.5	1	5.5	2	5.5	1
120;0.4	0.090	5.5	2	5.5	2	5.5	2
120;0.5	0.113	5.5	2	5.5	2	5.5	2
120;0.63	0.142	5.5	2	5.5	2	5.5	2
120;1.0	0.225	5.5	2	5.5	2	5.5	3
120;1.6	0.360	5.5	3	5.5	3	5.5	3

The image criteria score was shown in figure 4.3 to 4.5 and the qualitative noise score was shown in figure 4.6 to 4.8.

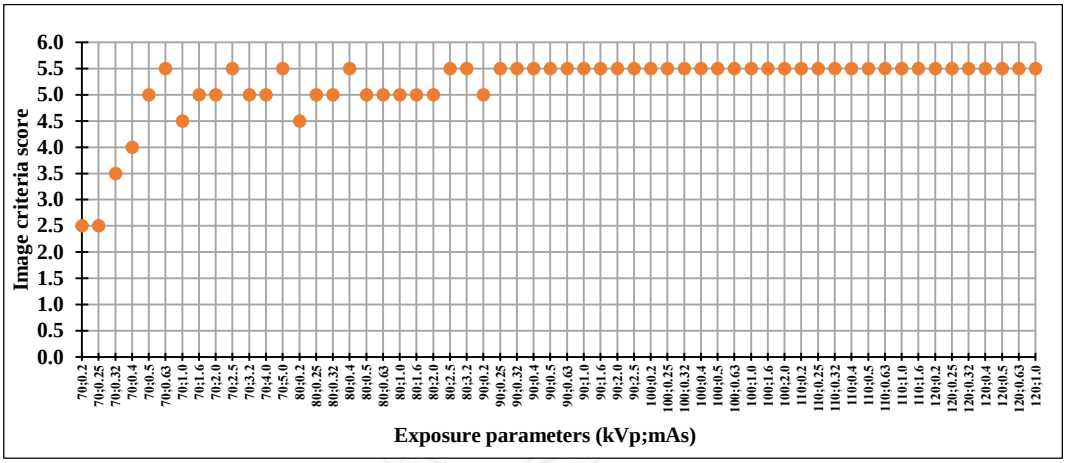

Figure 4.3 Scatter charts of image criteria score and exposure parameters by 1st observer.

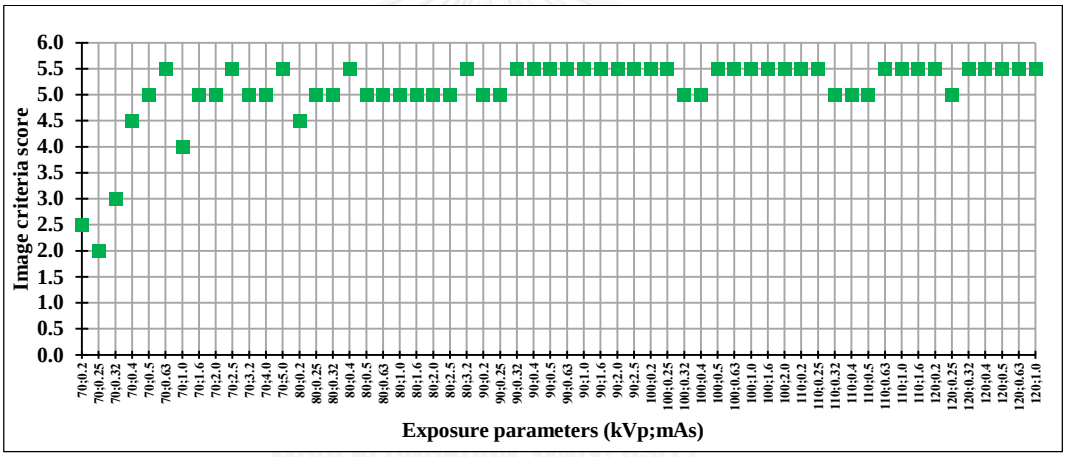

Figure 4.4 Scatter charts of image criteria score and exposure parameters by 2nd observer.

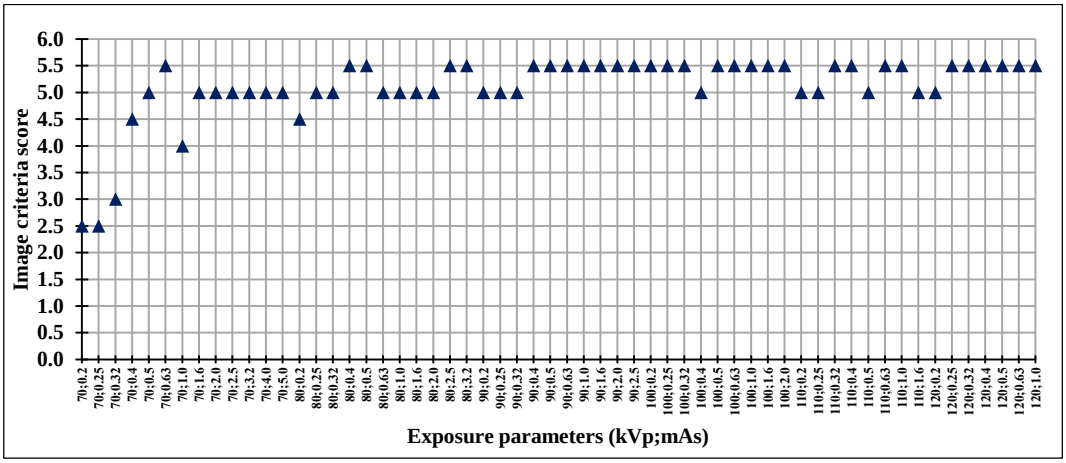

Figure 4.5 Scatter charts of image criteria score and exposure parameters by 3rd observer.

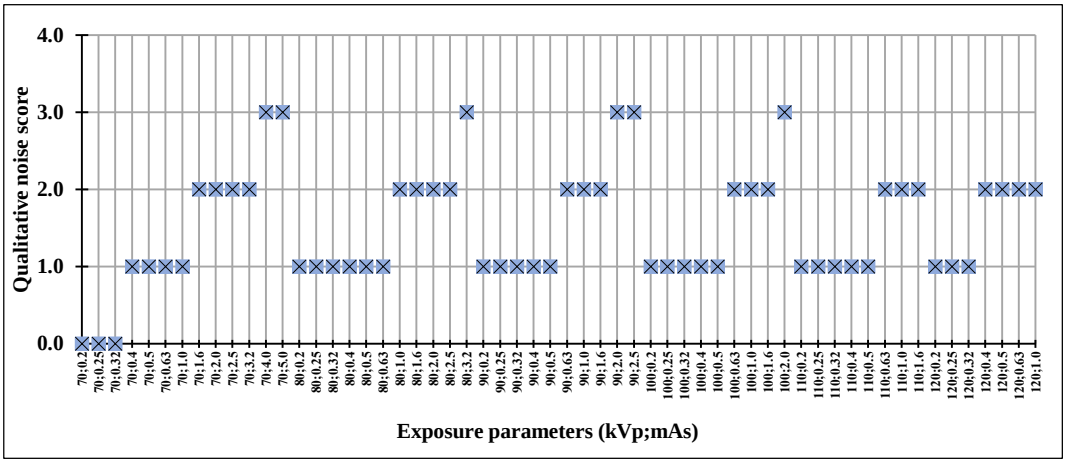

Figure 4.6 Scatter charts of qualitative noise score and exposure parameters by 1st observer.

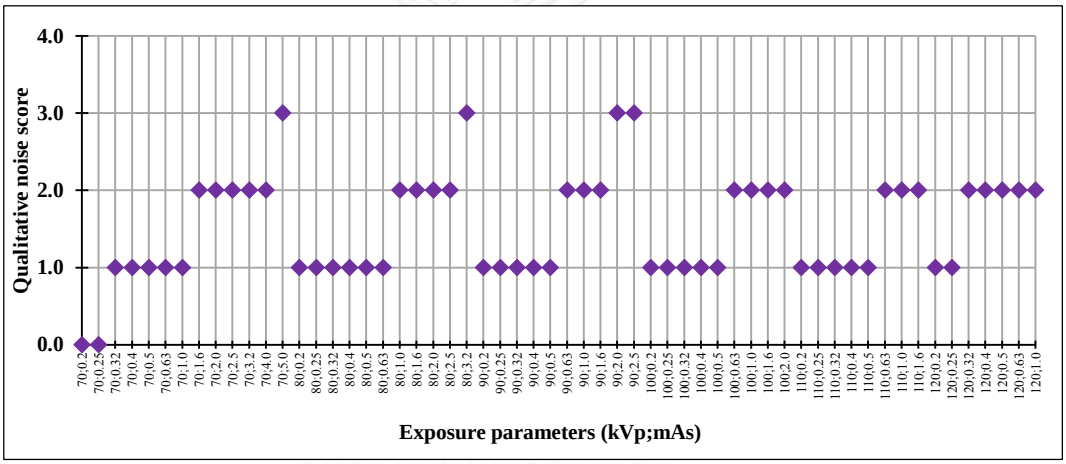

Figure 4.7 Scatter charts of qualitative noise score and exposure parameters by 2nd observer.

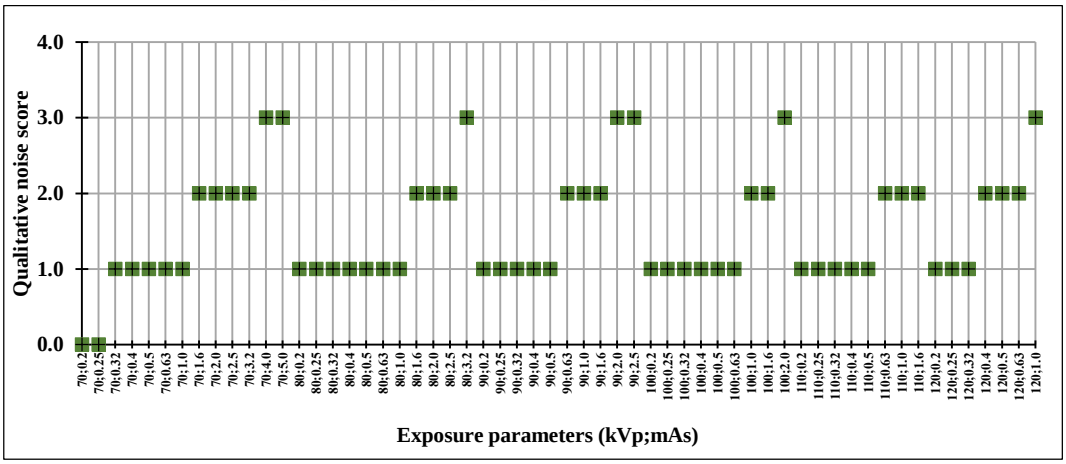

Figure 4.8 Scatter charts of qualitative noise score and exposure parameters by 3rd observer.

The image quality scored from three observers were compared as shown in figure 4.9, 4.10 and table 4.5. The range of image criteria and qualitative noise score were 2.5 to 5.5 and 0 to 3 respectively.

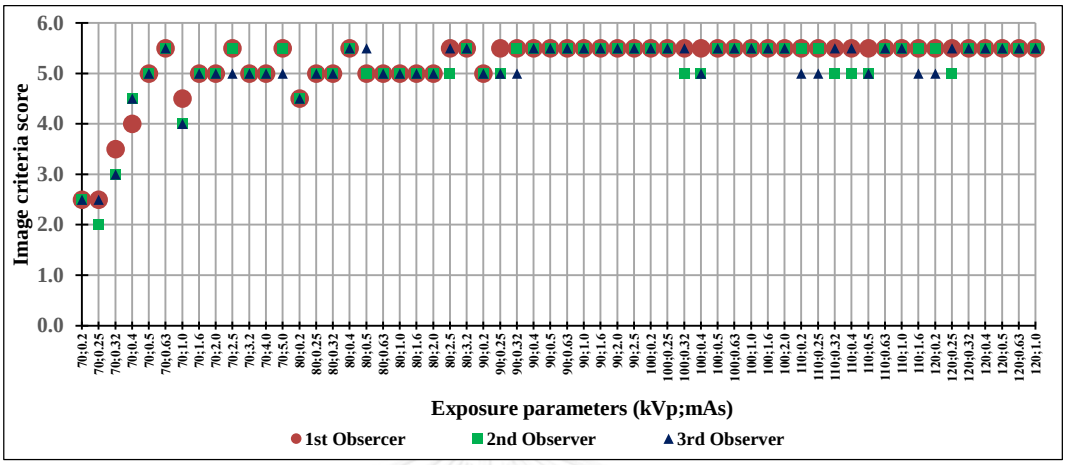

Figure 4.9 The image quality scored by three observers.

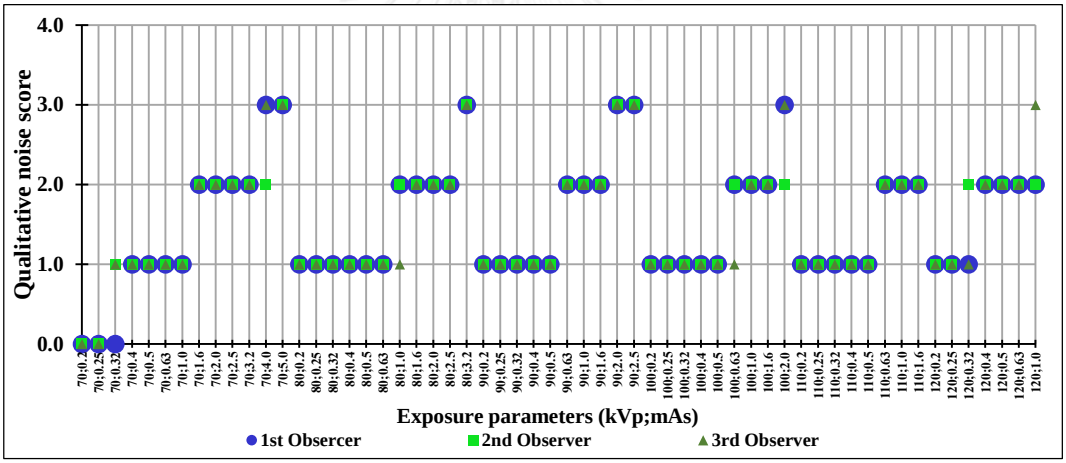

Figure 4.10 The qualitative noise scored by three observers.

Table 4.5 The observers' agreement

Observers	Kappa Value* (Image criteria)	Kappa Value* (Qualitative noise)
1st Observer and 2nd Observer	0.834	0.857
1st Observer and 3rd Observer	0.812	0.865
2nd Observer and 3rd Observer	0.775	0.725

* The kappa values were calculated using SPSS version 17.0

The classification of kappa value by Landis and Koch (1997) shows that the strength of agreement is excellent for 1st, 2nd and 3rdobservers. So, the optimal protocol has been developed from image quality scored by the 1stobserver.

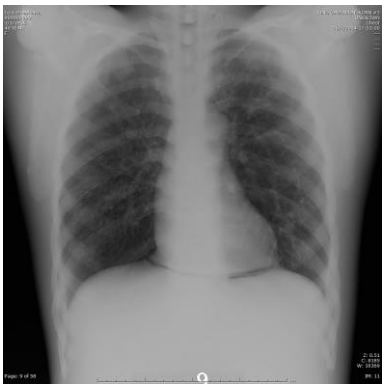

A) Score = 0 (Obvious noise)

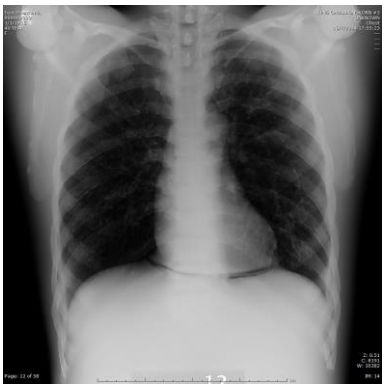

B) Score = 1 (Significant noise)

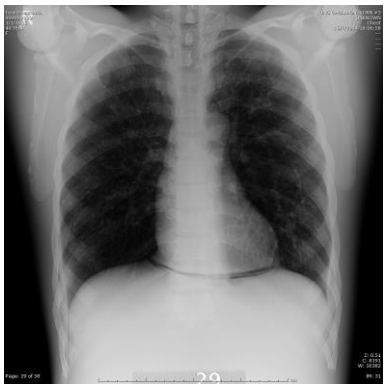

C) Score = 2 (Scarce noise)

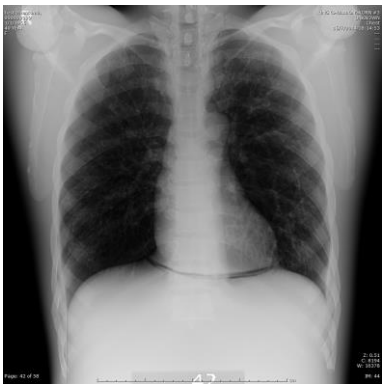

D) Score = 3 (Free of noise)

Figure 4.11 Classification of qualitative noise

4.5.3 Optimal protocol

The image quality scored by the 1st observer and the radiation dose (ESAK) were leading to the optimized protocol from the image criteria with score ≥ 5 and the qualitative noise score ≥ 2 as shown in table 4.6. Finally the optimal exposure parameter was kVp 90, mAs 0.63 and the ESAK was 0.083 mGy. The score on the image criteria and the qualitative noise were 5.5 and 2 respectively.

Table 4.6 The optimal protocol from the ESAK and image quality score

Exposure parameter :kVp; mAs	**ESAK (mGy)**	**Image quality (score)**	
		Image criteria	**Qualitative noise**
90;0.63	**0.083**	**5.5**	**2**
120;0.4	0.090	5.5	2
80;1.0	0.101	5.0	2
100;0.63	0.103	5.5	2
70;1.6	0.111	5.0	2
120;0.5	0.113	5.5	2
110;0.63	0.122	5.5	2
90;1.0	0.132	5.5	2
70;2.0	0.139	5.0	2
120;0.63	0.142	5.5	2
80;1.6	0.161	5.0	2
100;1.0	0.163	5.5	2
70;2.5	0.174	5.5	2
110;1.0	0.194	5.5	2
80;2.0	0.201	5.0	2
90;1.6	0.211	5.5	2
70;3.2	0.223	5.0	2
120;1.0	0.225	5.5	2
80;2.5	0.252	5.5	2
100;1.6	0.261	5.5	2
90;2.0	0.264	5.5	3
70;4.0	0.278	5.0	3
110;1.6	0.311	5.5	2
80;3.2	0.322	5.5	3
100;2.0	0.326	5.5	3
90;2.5	0.330	5.5	3
70;5.0	0.348	5.5	3
120;1.6	0.360	5.5	3
110;2.0	0.388	5.5	3

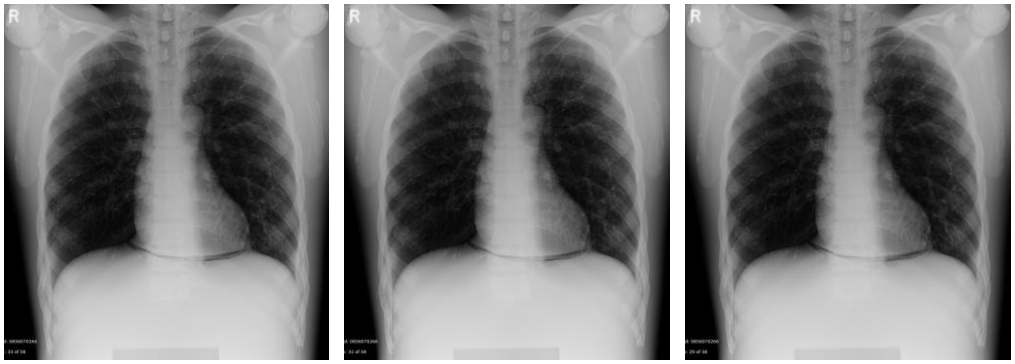

A) kVp 90 ; mAs 2.5
ESAK = 0.330 mGy
Image criteria = 5.5
Qualitative noise = 3

B) kVp 90 ; mAs 1.6
ESAK = 0.211 mGy
Image criteria = 5.5
Qualitative noise = 2

C) kVp 90 ; mAs 0.63
ESAK = 0.083 mGy
Image criteria = 5.5
Qualitative noise = 2

Figure 4.12 Phantom's radiographs from difference exposure parameters

4.6 Acceptable level for clinical diagnosis

For mobile digital chest radiography, the observers suggested the level of acceptance for diagnosis as;

4.5.1 Image criteria score ≥ 3

4.5.2 Qualitative noise ≥ 2

4.7 Patient study

Fifty patients of thirty-five male (70%) and fifteen female (30%) were exposed on chest by digital mobile x-ray system using the optimal protocol from the phantom study. The optimal protocol was kVp 90, mAs 0.63 and focus to image receptor distance 100 cm.

4.7.1 Patient dose (ESAK)

The patient ESAK was calculated using the x-ray tube output, tube loading and the chest thickness of patients. The results of ESAK and patient chest thickness were presented in table 4.7 and figure 4.13 to 4.15.

Table 4.7 Patient data and ESAK of the patient study

Case Number	Gender (M/F)	Chest thickness (cm)	ESAK (mGy)
1	M	22.0	0.081
2	M	18.0	0.073
3	M	19.0	0.075
4	M	22.0	0.081
5	F	18.0	0.073
6	M	16.0	0.070
7	M	18.5	0.074
8	F	23	0.083
9	F	17.5	0.072
10	F	16.0	0.070
11	F	19.0	0.075
12	M	22.0	0.081
13	F	16.5	0.070
14	M	18.0	0.073
15	M	19.0	0.075
16	M	21.0	0.079
17	F	20.0	0.077
18	M	22.5	0.082
19	M	17.0	0.071
20	M	21.0	0.079
21	F	20.0	0.077
22	M	19.0	0.075
23	M	21.0	0.079
24	M	22.5	0.082
25	M	23.0	0.083
26	M	23.0	0.083
27	M	17.5	0.072
28	M	19.5	0.076
29	M	17.5	0.072
30	M	22.0	0.081
31	F	17.0	0.071
32	F	20.0	0.077

Table 4.7 Patient data and ESAK of the patient study (Continued)

Case Number	Gender (M/F)	Chest thickness (cm)	ESAK (mGy)
33	M	22.0	0.081
34	F	20.0	0.077
35	M	20.0	0.077
36	M	17.0	0.071
37	M	19.0	0.075
38	M	23.0	0.083
39	F	21.0	0.079
40	M	21.0	0.079
41	M	19.0	0.075
42	M	18.0	0.073
43	F	20.0	0.077
44	M	20.0	0.077
45	M	20.0	0.077
46	M	18.0	0.073
47	M	23.0	0.083
48	F	18.0	0.073
49	F	19.0	0.075
50	M	19.0	0.075

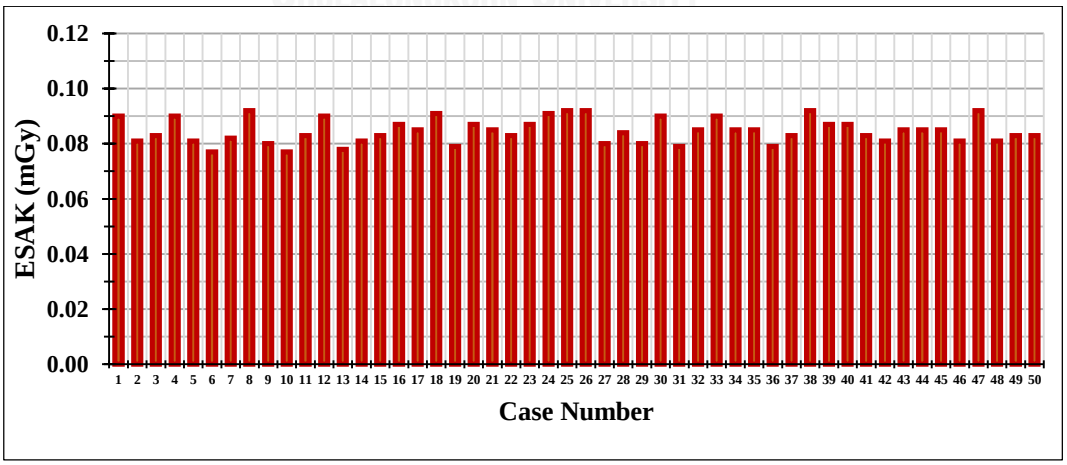

Figure 4.13 Bar charts of the ESAK, mGy for 50 patients.

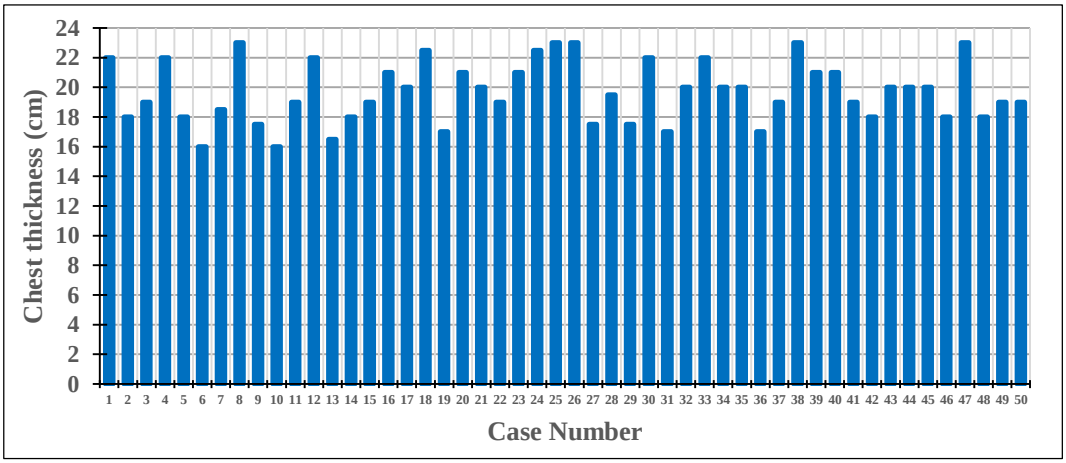

Figure 4.14 Bar charts of the patient chest thickness of 50 patients.

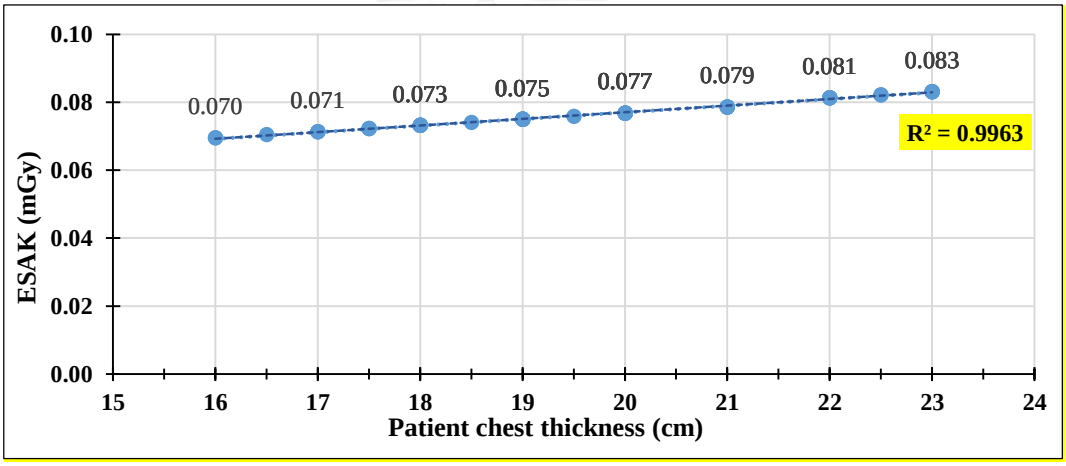

Figure 4.15 Graph of the patient chest thickness and patient dose (ESAK).

The average, range and S.D. of ESAK were 0.076 (0.070-0.083) ± 0.004 mGy and the average, range and S.D. of patient chest thickness were 19.7 (16-23) ± 2.03 cm as shown in table 4.8.

Table 4.8 Summary of patient dose and patient chest thickness

	Average	**S.D.**	**Minimum**	**Maximum**
Patient dose: ESAK (mGy)	0.076	0.004	0.070	0.083
Patient chest thickness (cm)	19.70	2.03	16.0	23.0

4.7.2 Image quality of patient study

The image quality of chest radiograph was evaluated by three observers using the same method of phantom study (4.4.2). The results of image quality were presented in table 4.9. The range of image criteria and qualitative noise score were 2.0 to 5.5 and 2 to 3 respectively.

Table 4.9 Image quality of the patient study

Case Number	1st Observer		2nd Observer		3rd Observer	
	Image criteria	Qualitative noise	Image criteria	Qualitative noise	Image criteria	Qualitative noise
1	3.5	2	3.0	2	3.5	2
2	4.0	3	4.0	3	4.0	2
3	4.0	2	4.0	2	4.0	2
4	3.5	2	3.5	2	3.5	2
5	4.5	3	4.5	3	4.0	3
6	4.5	3	4.5	2	4.5	2
7	5.0	3	5.0	3	5.0	3
8	3.5	2	4.0	2	4.0	2
9	4.0	3	4.0	3	4.0	2
10	3.5	3	3.5	3	3.5	2
11	3.0	2	3.0	2	3.5	2
12	4.5	2	4.5	2	4.5	2
13	2.5	3	2.5	3	2.0	3
14	2.0	3	2.0	2	2.0	3
15	3.0	2	2.0	2	3.0	2
16	5.0	2	5.0	3	5.0	2
17	3.5	2	3.5	2	3.5	2
18	3.5	2	3.5	2	3.5	2
19	3.5	3	3.5	3	4.0	3
20	2.0	2	2.0	2	2.0	2
21	3.5	2	3.5	2	3.5	2
22	4.0	2	4.0	3	4.0	2
23	4.5	2	4.5	2	5.0	2
24	3.5	2	3.5	2	3.0	2
25	2.0	2	3.0	2	2.0	2

Table 4.9 Image quality of the patient study (Continued)

Case Number	1st Observer		2nd Observer		3rd Observer	
	Image criteria	Qualitative noise	Image criteria	Qualitative noise	Image criteria	Qualitative noise
26	4.5	2	4.5	2	4.5	2
27	3.0	3	3.0	2	3.0	3
28	2.0	2	2.0	2	2.0	2
29	4.0	3	4.0	3	4.5	3
30	2.5	2	2.5	2	2.5	2
31	3.5	3	3.5	2	3.5	3
32	4.0	2	4.0	2	3.5	2
33	3.0	2	3.0	2	3.0	2
34	4.5	2	4.5	2	4.5	2
35	4.5	2	5.0	3	4.0	3
36	4.0	3	4.0	3	4.0	2
37	4.0	2	3.5	2	4.0	2
38	4.0	2	4.0	2	3.5	2
39	4.0	2	4.0	2	4.0	2
40	4.0	2	4.5	2	4.0	2
41	4.5	2	4.5	2	4.5	2
42	4.5	3	4.5	3	4.5	2
43	3.5	2	4.0	2	4.0	2
44	4.0	2	4.0	2	4.0	2
45	4.0	2	4.0	2	4.5	2
46	5.5	3	5.0	3	5.5	3
47	3.5	2	3.5	2	3.5	2
48	4.0	2	4.0	2	3.5	3
49	3.5	2	3.5	2	3.0	2
50	4.5	2	4.5	2	4.5	2

The image quality score compared with three observers as in table 4.10. Eighty eight percent of image criteria score was ≥ 3.0 and all of qualitative noise score was ≥ 2 (70% for score 2 and 30% for score 3). Figure 4.16 shows the image criteria and qualitative noise scores from the 1st observer.

Table 4.10 Overall image quality score of patient study

Image quality score	**1st Observer**	**2nd Observer**	**3rd Observer**
1. Image criteria			
0	-	-	-
0.5	-	-	-
1.0	-	-	-
1.5	-	-	-
2.0	4 (8%)	4 (8%)	5 (10%)
2.5	2 (4%)	2 (4%)	1 (2%)
3.0	4 (8%)	6 (12%)	5 (10%)
3.5	12 (24%)	11 (22%)	12 (24%)
4.0	15 (30%)	14 (28%)	14 (28%)
4.5	10 (20%)	10 (20%)	9 (18%)
5.0	2 (4%)	4 (8%)	3 (6%)
5.5	1 (2%)	-	1 (2%)
6.0	-	-	-
Total	**50 (100%)**	**50 (100%)**	**50 (100%)**
2. Qualitative noise			
0	-	-	-
1	-	-	-
2	35 (70%)	36 (72%)	39 (78%)
3	15 (30%)	14 (28%)	11 (22%)
Total	**50 (100%)**	**50 (100%)**	**50 (100%)**

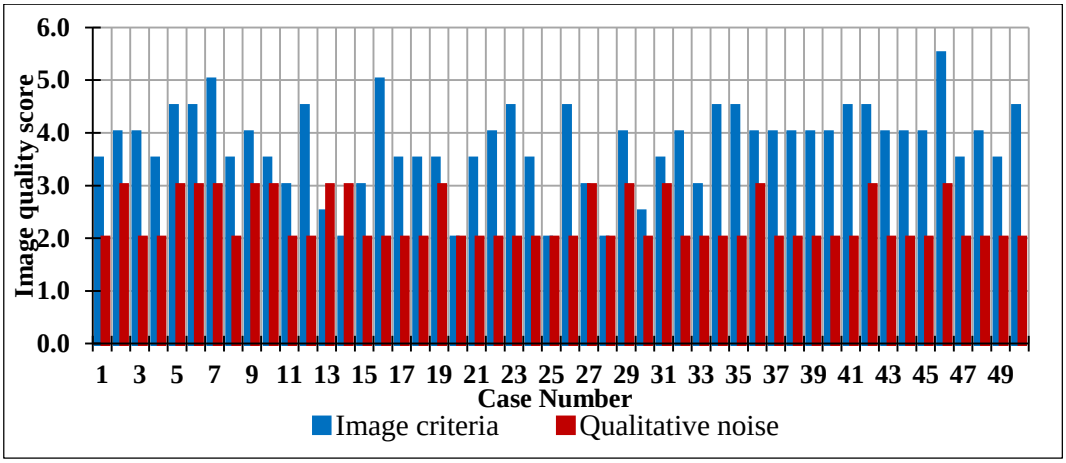

Figure 4.16 Bar chart of the image quality score of 50 cases

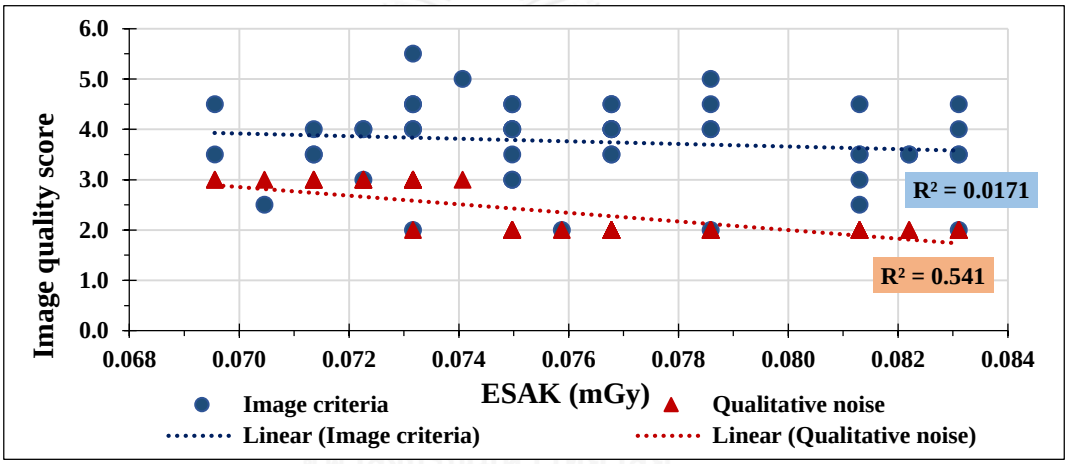

Figure 4.17 Scatter plot of the image quality score and patient dose (ESAK)

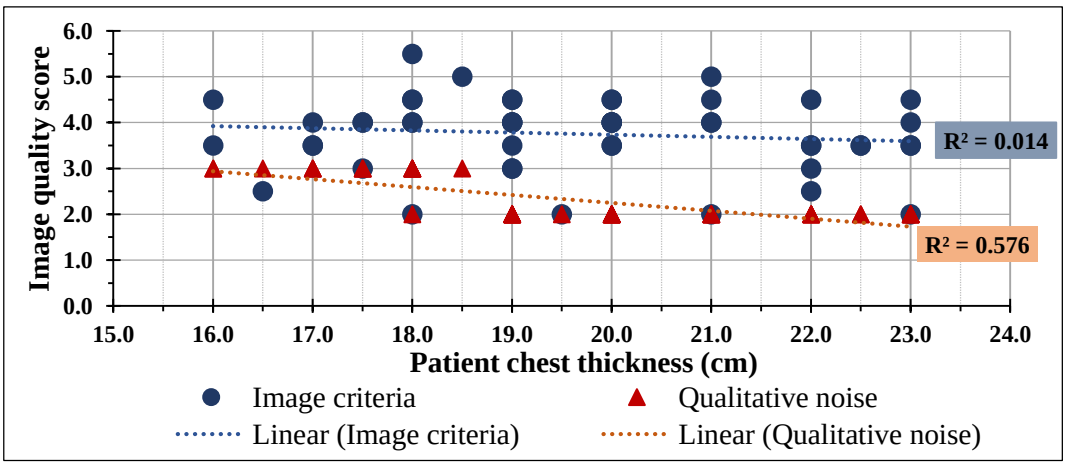

Figure 4.18 Scatter plot of the image quality score and patient chest thickness

4.7 Routine protocol

Collect ten patient's data exposed by digital mobile x-ray system of routine protocol retrospectively. The results of using routine protocol were presented in table 4.11.

Table 4.11 Patient data, ESAK and image quality score using routine protocol.

Case Number	Gender (M/F)	Chest thickness (cm)	Exposure parameter :kVp;mAs	ESAK (mGy)	Image quality	
					Image criteria	Qualitative noise
1	M	22.5	90;2.5	0.326	4.0	3
2	M	15.0	85;2.0	0.212	4.0	3
3	M	22.0	95; 1.6	0.206	2.5	3
4	M	20.0	85;1.6	0.191	3.5	3
5	F	19.0	90;0.8	0.096	2.0	2
6	M	21.0	90;1.0	0.126	4.0	2
7	M	18.0	90;1.0	0.117	5.0	3
8	F	19.0	95;1.6	0.191	4.0	3
9	F	23.0	100;2.0	0.265	4.5	3
10	F	19.0	95;1.6	0.191	3.5	3

In routine protocol, the average, range and S.D. of ESAK were 0.192 (0.096-0.326) ± 0.069 mGy and the average, range and S.D. of patient chest thickness were 19.85 (15-23) ± 2.40 cm as shown in table 4.12.

Table 4.12 Summary of patient dose and patient chest thickness of the routine protocol

	Average	S.D.	Minimum	Maximum
Patient dose: ESAK (mGy)	0.192	0.069	0.096	0.326
Patient chest thickness (cm)	19.85	2.40	15.0	23.0

The range of image criteria score and qualitative noise score were 2.0 to 5.0 and 2 to 3 respectively as shown in table 4.13. Eighty percent of image criteria score was ≥ 3.0 and all of qualitative noise score was ≥ 2 (20% for score 2 and 80% for score 3).

Table 4.13 Overall image quality scored by first observer of routine protocol

	Image quality score	**1st Observer**
1.	Image criteria	
	0	-
	0.5	-
	1.0	-
	1.5	-
	2.0	1 (10%)
	2.5	1 (10%)
	3.0	-
	3.5	2 (20%)
	4.0	4 (40%)
	4.5	1 (10%)
	5.0	1 (10%)
	5.5	-
	Total	**10 (100%)**
2.	Qualitative noise	
	0	-
	1	-
	2	2 (20%)
	3	8 (80%)
	Total	**10 (100%)**

4.8 Comparison of optimal protocol to routine protocol

The patient dose and image quality using routine protocol and optimal protocol in terms of number of patient, patient chest thickness, patient dose (ESAK) and image quality score were presented in table 4.14.

Table 4.14 The number of patients and demography, the Image quality scores in optimal and routine protocols

	Routine protocol	**Optimal protocol**
Number of patients	10	50
Patient chest thickness (cm)	19.85 (15-23)	19.70 (16-23)
Patient dose (mGy)	0.192±0.069	0.076±0.004
Image criteria score	≥ 3.0 (80%)	≥ 3.0 (88%)
Qualitative noise score	2 (20%), 3 (80%)	2 (30%), 3 (70%)

Chest radiographs of the same patient were exposed by routine and optimal protocol shown in figure 4.19.

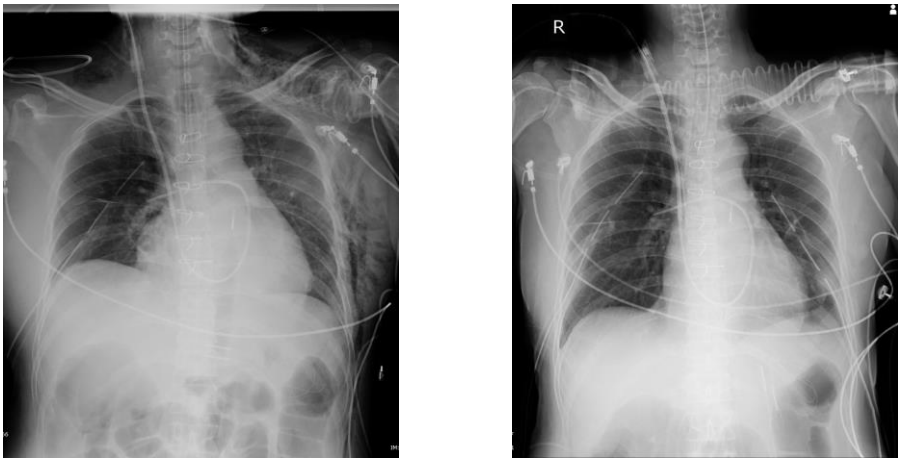

A) Routine protocol B) Optimal protocol

Figure 4.19 Chest radiographs from routine and optimal protocol

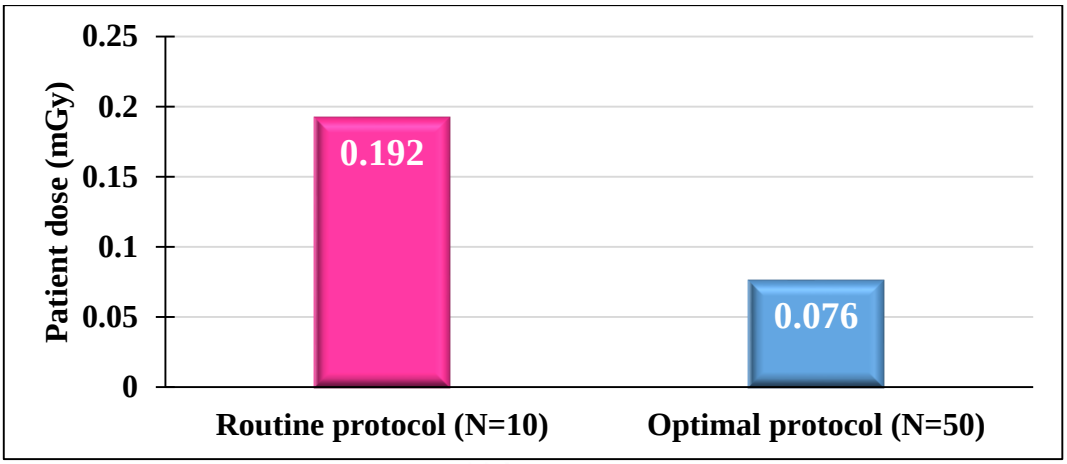

Figure 4.20 The patient dose (ESAK) using routine and optimal protocols.

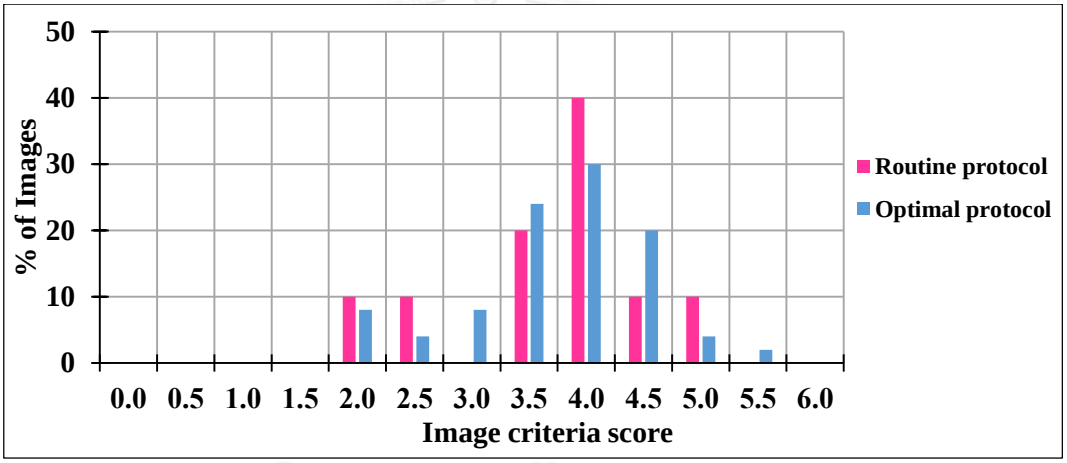

Figure 4.21 Image criteria score using routine and optimal protocols

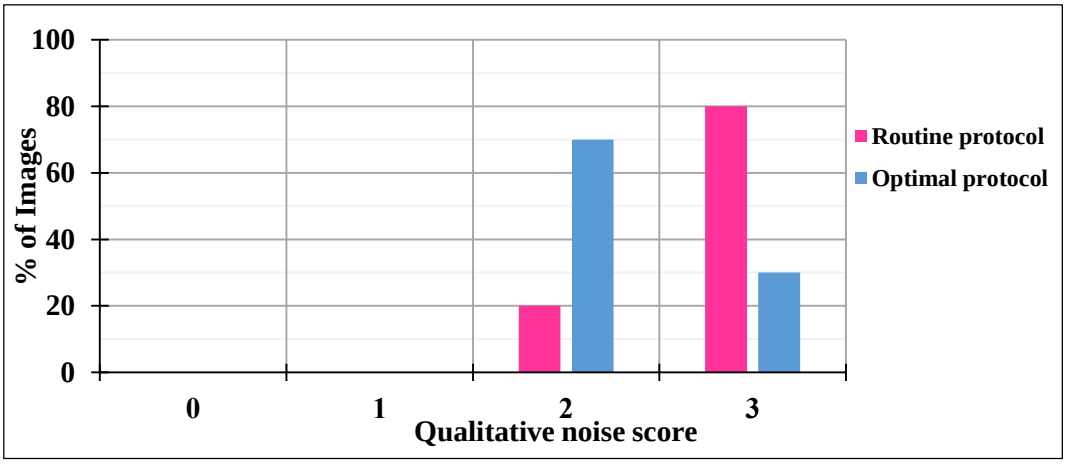

Figure 4.22 Qualitative noise score using routine and optimal protocols

Using the optimal protocol, the average of ESAK reduced to 0.076 mGy. A reduction of 60% from the routine protocol. The image criteria score of the optimal protocol (88%) and routine protocol (80%) were ≥ 3. The qualitative noise score of the optimal protocol (70%) and routine protocol (20%) were 2, optimal protocol (30%) and routine protocol (80%) were 3. All of the image quality was assessed to be acceptable for diagnosis.

CHAPTER 5
DISCUSSION AND CONCLUSION

5.1 Discussion

For the estimation of the patient radiation dose, measurement of the ESAK was required with the evaluation of absorbed dose to individual organs. ESAK depends on the x-ray tube output (kVp.), tube loading (mAs) and chest thickness of patient. The ESAK increases as kVp, mAs and chest thickness increase. ESAK had been calculated for 96 exposure parameters from kVp 70 to 120, mAs 0.2 to 10 and the phantom thickness 23 cm with the range of 0.014 to 2.252 mGy.

In the phantom study of AP projection, 60 exposure parameters were obtained when the ESAK was lower than 0.4 mGy with the range of 0.014 to 0.388 mGy. The criteria for determining the quality of the radiographs included image criteria of chest radiography standard in PA upright position based on the CEC was adjusted to 6 items. The image noise that appeared on the radiographs was also determined. The criterion to determine the optimal protocol consists of the score of image criteria equal to or more than 3 and qualitative noise equal to or more than 2.

From the phantom study, 29 exposure parameters met the criteria of the optimal protocol. The results of phantom study lead to the optimal protocol of kVp 90 and mAs 0.63 evaluate from optimization between image criteria score was 5.5 from 6, qualitative noise score was 2 from 3 and radiation dose (ESAK) was 0.083 mGy.

Disadvantages of chest radiography using mobile x-ray unit is the low image quality because it was taken in AP supine position but it is also useful for the treatment by physicians. Therefore, it is necessary to define criteria for mobile chest radiography. In this study, the observers had suggested a level of acceptance criteria of mobile chest radiography for clinical diagnosis follows the score of image criteria equal to or more than 3 and qualitative noise score equal to or more than 2.

Ten patients of six male and four female were exposed by routine chest protocol using digital mobile x-ray. The average patient chest thickness was 19.85 cm, range from 15 to 23 cm. The average patient dose (ESAK) was 0.192 mGy and range from 0.096 to 0.326 mGy. 80% of image criteria score was ≥ 3.0 and all of qualitative noise score was ≥ 2 (20% for score 2 and 80% for score 3).

Fifty patients of thirty five male and fifteen female were exposed using optimal protocol from the phantom study. The average patient chest thickness was 19.70 cm, range from 16 to 23 cm. The average patient dose (ESAK) was 0.076 mGy and range from 0.070 to 0.083 mGy. 88% of image criteria score was ≥ 3.0 and all of qualitative noise score was ≥ 2 (70% for score 2 and 30% for score 3). The scores of image criteria varied from 2.0 to 5.0 due to pathology or patient's disease result in lower score. The score on qualitative noise was 2 or 3, which correspond to the phantom study.

Before the study, the average patient dose using routine protocol was 0.192 mGy. When the optimal protocol was implemented, the average patient dose reduced to 0.076 mGy, a reduction by 60%. Assessment of image quality found no difference.

Due to the average of patient chest thickness at King Chulalongkorn Memorial Hospital was 19 cm, smaller than the western standard. According to the protocol at the Department of Radiology the anti-scatter grid had not been used for chest radiography in AP supine position. The size of collimator depends on the size of each patient. Hence the anti-scatter grid and collimation had not been used in this study.

Coblentz [21] recommended the kilo-voltage between 80 and 90 and 125 cm of focus to image receptor distance used for mobile chest radiography in semi-erect or supine position. Our study suggested kVp 90 for mobile chest radiography in semi-erect or supine position at 100 cm of focus to image receptor distance.

Furthermore, figure 4.16 showed that when the patient chest thickness was less than 19 cm, the score of qualitative noise was approximately 3, which represented low noise or free of noise on the radiographs. Follow the criteria to determine the optimal protocol in terms of the qualitative noise score was equal to or more than 2 (scarce of noise), which acceptable to use to diagnostic.

The optimal protocol of the study is particularly useful for patients who have exposed several times by mobile chest radiography during the period of treatment in the hospital. As a result, patients received radiation dose greater than necessary with increasing radiation risk. The optimal protocol reduces the unnecessary radiation to chest radiography patients more than half of the radiation dose from the previous protocol without affecting the clinical image quality.

5.2 Conclusion

The optimal protocol to optimize the radiation dose and image quality for chest radiograph using digital mobile x-ray system at the In Patient Department (IPD), King Chulalongkorn Memorial Hospital was kVp 90 and mAs 0.63 at 100 cm of Focus to Image receptor distance (FID), suitable for the thickness of chest equal to or less than 23 cm.

Mobile chest radiography using the optimal protocol was assessed to be acceptable for diagnosis. Including the acceptable score of image criteria was equal to or more than 3 from 6 items and the acceptable score of qualitative noise was equal to or more than 2 from 3 levels (scarce noise or free of noise).

As the average patient dose for routine chest study was 0.192 mGy, the patient doses using optimal protocol was 60% less than routine study and also lower than the International Atomic Energy Agency dose reference level of 0.4 mGy for chest radiography.

5.3 Recommendation

Future studies should be extended for different sizes of phantom, suitable for use in the different patient sizes. The exposure parameter might be adjusted by reducing kVp and mAs, which directly affects the patient dose and increasing image noise but remains acceptable to diagnostic.

This research is preliminary study for the other examination when using digital mobile x-ray system according to IAEA recommendation such as skull, plain abdomen supine, lumbar spine and pelvis.

REFERENCES

1. Tracy LH, Terri LF, Julie G, Colleen H, Denise K. Prouty BS, Andrew P. W, et al. Best Practices in Digital Radiography. American Society of Radiologic Technologists. 2012:1-20.
2. Markus K, Christof HW, Stefan W, Kluas-Jurgen P, Maximilian FR, Marcus T. Advances in Digital Radiography-Physical Principles and System Overview. RadioGraphics. 2007;27:675-86.
3. Rubinowitz AN, Siegel MD, Tocino I. Thoracic Imaging in the ICU. Critical Care Clinics. 2007;23(3):539-73.
4. Kotter E, Langer M. Digital radiography with large-area flat-panel detectors. European radiology. 2002;12(10):2562-70.
5. Lança L, Silva A. Digital radiography detectors – A technical overview: Part 1. Radiography. 2009;15(1):58-62.
6. Chotas HG, Dobbins JT, Ravin CE. Principles of digital radiography with large-area, electronically readable detectors: a review of the basics. Radiology. 1999;210(3):595-9.
7. Cha BK, Lee SJ, Muralidharan P, Kim DK, Kim JY, Cho G, et al. Novel nanocrystalline Gd2O3(Eu) scintillator screens with a micro-pixel structure for high spatial resolution X-ray imaging. Nuclear Instruments and Methods in Physics Research Section A: Accelerators, Spectrometers, Detectors and Associated Equipment. 2011;652(1):717-20.
8. Williams MB, Krupinski EA, Strauss KJ, Breeden WK, Rzeszotarski MS, Applegate K, et al. Digital radiography image quality: image acquisition. Journal of the American College of Radiology : JACR. 2007;4(6):371-88.
9. Thulani N. Dose optimization in diagnostic radiology. Johannesburg: Witwatersrand; 2012.
10. Andriole KP, Ruckdeschel TG, Flynn MJ, Hangiandreou NJ, Jones AK, Krupinski E, et al. ACR-AAPM-SIIM practice guideline for digital radiography. Journal of digital imaging. 2013;26(1):26-37.
11. Keawsamur M. Optimal protocol of single-shot dual energy subtraction chest radiography: Chulalongkorn; 2012.
12. William RR. Image quality in chest radiography. American Association of Physicsts in Medicine, 2004.
13. Anders T. Quantifying the quality of medical x-ray images. Sweden: Lund; 2000.
14. Coblentz C, Matzinge F, Samson L, Scherer J, Strolberg H, Weisbrod G. Standard for Chest Radiography. Canadian Association of Radiologists, 2000.
15. Sun Z, Lin C, Tyan Y, Ng KH. Optimization of chest radiographic imaging parameters: a comparison of image quality and entrance skin dose for digital chest radiography systems. Clinical imaging. 2012;36(4):279-86.

16. Anderson DW. Introduction of grids to mobile ICU radiography in a teaching hospital. British Journal of Radiology. 2006;79:315-18.
17. Schaefer-Prokop C, Neitzel U, Venema HW, Uffmann M, Prokop M. Digital chest radiography: an update on modern technology, dose containment and control of image quality. European journal of radiology. 2008;18:1818-30.
18. American Association of Physicist in Medicine. Report No.74 quality control in diagnostic radiology. The American Association of Physicist in Medicine,2002.
19. King's College Hospital. KCARE protocol for the QA of Direct Digital Radiographt System Commissioning and Annual QA Test. King's Center for the Assessment of Radiological Equipment, King's College Hospital,2004.

APPENDIX

Appendix A: Report of Digital X-ray system performance

General Information

Location:	King Chulalongkorn Memorial Hospital
Date:	29/06/2014
Equipment number:	3
Manufacturer:	General Electric Company (September 2013)
Model number:	5555000-6 (Optima XR220amx)
Serial number:	1031650WK3

Checklist

P General mechanical and electrical condition

P Tube angle indicator, tube motion and locks

P Focus to film distance indicator (SID)

P Field size indicator

P Congruency of light and radiation fields

P Crosshair centering

P Focal spot size

N/A Photo cell consistency

N/A Bucky/Grid Centering

N/A Automatic Collimation (PBL)

P Beam quality (Half Value Layer)

P Consistency of exposure (mGy/mAs)

P kVp Accuracy

N/A Timer accuracy

P mA or mAs Linearity

N/P ESE calculations

N/A Relative radiation wave form

P Exposure repeatability

N/P Reciprocity

P = Performed

N/P = Not Performed

N/A = Not Application

General Condition of Mechanical and Electrical Components

N Are there any frayed or exposed electrical wires?

N Could electrical wires interfere with the use of the unit?

N/A Is there play in the couch when it is locked?

N/A Does it have the freedom of movement it was designed for?

N/A Is the couch level in tube and perpendicular directions?

N Is there play in the tube when it is locked?

Y Does it have the freedom of movement it was designed to have?

Y Does the visual, and/or, audible beam-on indicator function?

N Is the dead man switch installed correctly?

Target to Film Distance Indicator Check (at 100 cm SID)

SID: **100** cm. Allowable limit = ±2% SID

Measured distance: **99.5** cm.

Indicated distance: **100** cm.

Radiographically (determined) distance: - cm.

% Difference: **0.50%**

Pass or Fail: Pass

Tube Angle Indicator Check

CW:		**CCW:**	
0°:	**0°**		
45°:	**45°**	45°:	**45°**
90°:	**90°**	90°:	**90°**

Allowable limit = ±5° Pass/Fail: **Pass**

Motion and Lock Check

	Motion	**Locks**
Tube longitudinal:	**Yes**	**Yes**
Tube Rotate:	**Yes**	**Yes**
Tube Transverse:	**Yes**	**Yes**
Tube Vertical:	**Yes**	**Yes**
Tube Angulate:	**Yes**	**Yes**
Collimator Jaws:	**Yes**	**Yes**
Collimator	**Yes**	**Yes**

Field Size Indication

Purpose: to insure that the radiographer can set a desired field size using the light field collimator.

Requirement: ± 2% SID.

SID: **100** cm.

Indicator Setting	Measured Longitudinal	Measured Transverse	% Variation	Pass/Fai
18 x 18	17.37	17.54	0.63%	Pass
25 x 25	24.42	24.77	0.58%	Pass
35.6 x 35.6	34.73	35.14	0.87%	Pass

Congruence of Light and Radiation Fields

Purpose: to determine the alignment of the light and radiation fields.

Requirement: alignment to within ± 2% of indicated SID.

Method: mark corners of light field and compare to radiation field.

SID: **100** cm.

Field Size	Light Field Size		Radiation Field Size		%Variation	Pass
	Measured Longitudinal	Measured Transverse	Measured Longitudinal	Measured Transverse		/Fail
18 x 18	17.37	17.54	16.90	17.72	0.47%	Pass
25 x 25	24.42	24.77	24.13	25.16	0.39%	Pass
35.6 x 35.6	34.73	35.14	35.02	36.07	0.93%	Pass

Focal Spot Size

Purpose: to determine the size of the focal spot at a known technique with a view to detect degradation of the focal spot.

Method: Siemens star technique.

	Set kVp:	50	Set mAs: 12.5		
Degree of Star:		2	Large or Small Focal Spot:	**Large**	
Star dimension:					
Actual:	55	mm.	Radiographic:	107.04	mm.
Blurr:	42.81	mm.	Manufacturer specification:	1.2	
Computed Focal Spot Size:		**1.58**	Meets NEMA: **Yes**		

	Set kVp:	50	Set mAs: 1.6		
Degree of Star:		2	Large or Small Focal Spot:	**Small**	
Star dimension:					
Actual:	55	mm.	Radiographic:	107.14	mm.
Blurr:	18.73	mm.	Manufacturer specification:	0.6	
Computed Focal Spot Size:		**0.69**	Meets NEMA: **Yes**		

Cross Hair Centering

Purpose: to determine if the light field cross hair indicates the central axis of the x-ray beam.

Requirement: must be within ± 2% of indicated SID.

SID: **100** cm.

Deviation between radiation and optical field center: 0.4 cm.

Indicate Field size (cm)	Deviation (cm)	%Deviation
18 x 18	0.4	0.4
25 x 25	0.3	0.3
35.6 x 35.6	0.4	0.4

Pass/Fail: **Pass**

Beam Quality (Half Value Layer)

Method: set 80 kVp.

Requirement: - NCRP#33 recommends not less than 2.3 mmAl at 80 kVp.
– AAPM recommends not less than 2.5 mmAl at 80 kVp.

Filter (mmAl)	Instrument Reading (mGy)
OPEN	2.491
1.0	1.957
2.0	1.591
3.0	1.331
3.5	1.221

Calculated HVL: **3.39** mmAl

Pass/Fail: **Pass**

Exposure Consistency

Purpose: to determine if the exposure is remaining consistent.

Requirement: coefficient of variation should be ≤ 0.05.

Set SCD: **66** cm. Set kVp: **80** Field size: **10 x 10** cm.

Set mAs: **25**

	kVp	Time (ms)	Dosimeter (mGy)	DAP meter (mGy)
	82.29	82.00	2.48	2.47
	82.18	82.22	2.48	2.47
	82.16	82.11	2.48	2.49
	82.14	82.00	2.47	2.50
Mean	**82.19**	**82.11**	**2.48**	**2.48**
Std.Dev.	0.058	0.090	0.002	0.013
C.V.	0.001	0.001	0.001	0.005

Pass/Fail: **Pass**

mA or mAs Linearity

Method: select 80 kVp vary mAs from 0.5 to 50 and record the exposure in mGy

Requirement: coefficient of variation should not exceed 0.1

Set SCD: **66** cm. Phase: **1** Set kVp: **80**

S/L	Avg. kVp	Time (msec)	mAs	DAP (mGy)	Dosimeter (mGy)	mGy/mAs	C.V.
S	-	4.22	0.5	0.05	0.05	0.098	-
S	-	5.56	1.0	0.10	0.10	0.098	0.001
S	82.94	10.77	2.0	0.20	0.20	0.100	0.008
S	83.20	21.66	4.0	0.40	0.40	0.100	0.002
S	82.67	59.00	8.0	0.80	0.81	0.101	0.004
S	82.42	84.88	10.0	1.02	1.01	0.101	0.000
L	81.93	41.00	12.5	1.23	1.23	0.099	-0.013
L	82.27	65.77	20.0	1.98	1.98	0.099	0.001
L	82.08	82.33	25.0	2.47	2.47	0.099	0.000
L	82.07	105.50	32.0	3.16	3.16	0.099	0.000
L	82.05	132.20	40.0	3.95	3.96	0.099	0.000
L	82.19	169.60	50.0	4.94	4.95	0.099	0.000

Global Mean: **0.099**

Global Std.Dev: **0.001**

Global C.V: **0.010**

Pass/Fail: **Pass**

kVp Linearity

Method: at a mid-current station, vary the kVp from minimum to maximum in step of 10 kVp. Record the measured kVp

Requirement: the deviation should not exceed 5 kVp or 10% of set kVp, whichever is larger. (5% of set kVp for new equipment)

Set SCD: **66** cm. Phase: **1** Set mAs: **25**

Set kVp	Measured kVp		DAP (mGy)	Dosimeter		
	Avg.	%Dev.		HVL (mmAl)	(mGy)	mGy/mAs
50	49.60	0.80	0.75	2.14	0.81	0.03
60	60.35	0.58	1.27	2.51	1.30	0.05
70	71.01	1.44	1.83	2.93	1.84	0.07
80	82.28	2.85	2.47	3.38	2.47	0.10
90	92.64	2.93	3.13	3.88	3.16	0.13
100	103.20	3.20	3.84	4.35	3.91	0.16
110	114.10	3.73	4.54	4.81	4.72	0.19
120	124.70	3.92	5.31	5.24	5.57	0.22

Pass/Fail: **Pass**

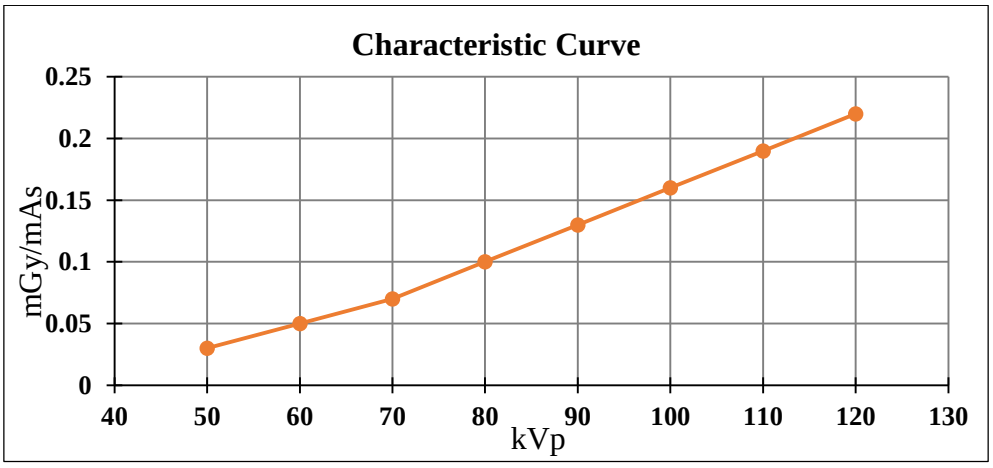

Appendix B: Report of Digital Radiography system performance

General Information

Location:	King Chulalongkorn Memorial Hospital
Date:	14/07/2014
Detector number	3
Manufacturer:	General Electric (GE) ; June 2013
Model number:	5340000-7
Serial number:	UA45948-6

Commissioning Tests

Objective:

- To assess digital detector performance.

Equipment:

1. Tape measure
2. Adhesive tape
3. 1.5 mm Cu filtration (>10x10 cm)
4. Dosimeter Unfors Raysafe model Xi
5. TO20 threshold contrast test object
6. Resolution test object (Huttner 18)
7. M1 geometry test object
8. Lead glass phantom (10x10 cm)

The tests should be performed X-Ray unit and workstation that machines passed QC tests. These tests require the use of the higher quality reporting workstation like a clinical workstation.

Quality Assurance of Digital Detector

1. Dosimetry

Purpose: To measure entrance receptor doses required for later test.

Method:

1. Set SID at 180 cm.
2. Set SCD at 30.7 cm. in front of detector.
3. Collimate to the dosimeter.
4. Exposed the chamber such that the inverse square law corrected dose to the chamber is approximately 10 µGy, using 75 kVp, and 1.5 mmCu filtration.
5. Record the measured dose and repeat twice.
6. Under the same beam conditions determine the mAs required to deliver 1 µGy, 4µGy, 12µGy and 50µGy.

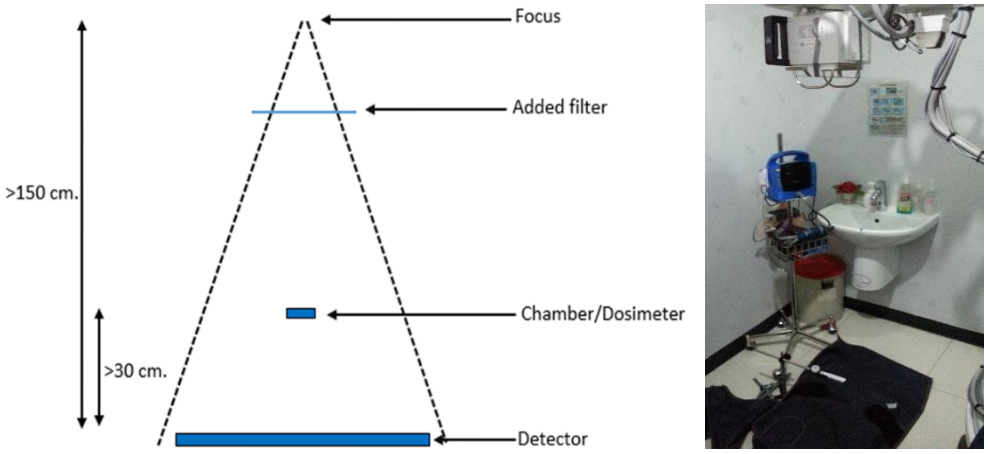

Figure 1: Set up for Dosimetry

Result:

Table 1: The mAs was create receptor dose at 4 µGy, 10 µGy, 12 µGy, 50 µGy

Radiation dose (µGy)	SCD (cm)	kV	Time (msec.)	mAs	Measured dose at dosimeter (µGy) (SCD)	Calculated dose at detector (µGy) (SID)
1	159	75	-	4	1.32	1.03
4	159	75	3.072	16	5.33	4.16
10	159	75	4.813	40	13.54	10.56
12	159	75	6.042	50	17.03	13.29
50	159	75	22.12	200	69.33	54.09

2. Linearity and system transfer properties

Purpose: To establish the relationship between receptor dose and pixel value so that this relationship can be corrected for in image retention and uniformity tests.

Method:

1. Remove grid from system.
2. Expose the entire area of the detector at 75 kVp with 1.5 mmCu. Set a 4.0 mAs and SID to deliver a dose of 1µGy.
3. Record the sensitivity index value (EI).
4. Repeat for doses of order 4 µGy, 10 µGy, 12 µGy and 50 µGy.
5. Record a pixel value from the center the image.

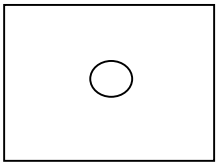

Figure 2: Position for measurement pixel value.

6. Plot a graph of pixel value versus receptor dose using a graph plotting. Obtain the equation of the trend-line for this graph (the pixel value as a function of receptor dose).

Result:

Table 2: Pixel values at center of image and receptor dose

kVp.	mAs	Dose(μGy)	Pixel Value (Center of image)	
			Mean	Std Dev.
75	4	1	266.07	4.78
75	16	4	1087.99	9.44
75	40	10	2742.00	16.40
75	50	12	3431.91	18.55
75	200	50	13761.62	46.85

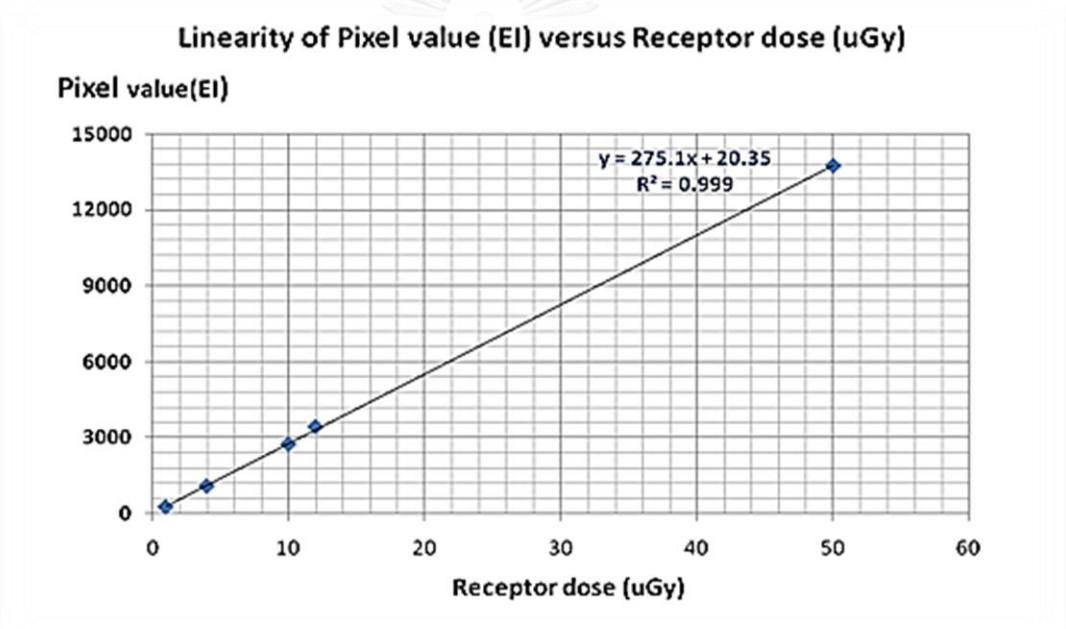

Figure 3: Relation graph between pixel value and receptor dose

Tolerance:

The trend-line plotted in excel should have an R^2 fit value >0.95. ($R^2 = 0.999$)

There is no tolerance for the STP equation. However the pixel value to dose relationship should be a simple relationship.

Pass/Fail: Pass

3. Image retention

Purpose: To test that any detectable residual signal (ghosting) that remains in subsequent images is minimal.

Method:

1. Remove grid from system and ensured that there is no attenuation in the beam.
2. Set the focus to detector distance (SID) to be 180 cm.
3. Close the collimators and cover the detector with a lead apron. Set a low exposure 50 kVp and 0.5 mAs.

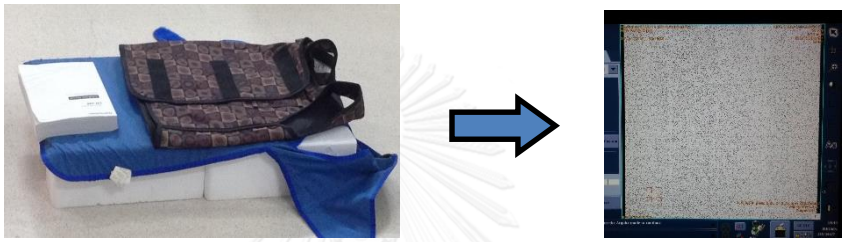

Figure 4: Close detector with a lead apron and image after exposure

4. Open the collimators and place the attenuating material-Lead glass 10x10 cm^2 on the detector. Make an exposure at 70kVp and 16 mAs to deliver a receptor dose of 4 µGy.

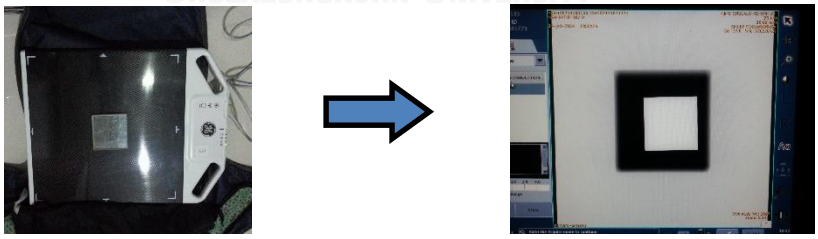

Figure 5: Lead glass and image after exposure

5. Obtain another blank image as described in step 3.
6. Set a very narrow window and adjust the level. Visually inspect the image for any remnant of the previous image. If a remnant is visible, use region of interest analysis to quantify the difference in pixel value between the ghosted and unghosted areas.

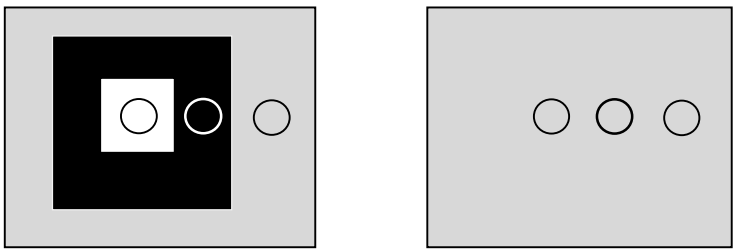

Figure 6: Region of interest for image retention

Result:

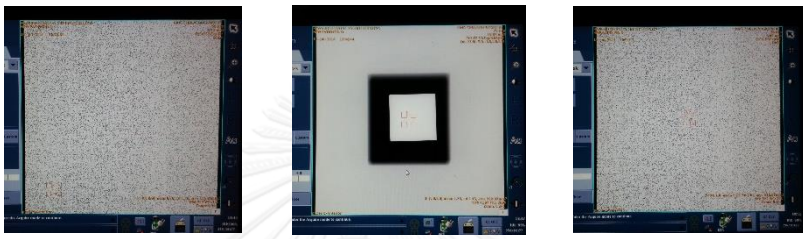

(a) (b) (c)

Figure 7: Compare Images from Step 3(a), Step 4(b) and Step 5(c)

Table 3: Ghosting artifact in each exposure technique

Image	kV	mAs	Material on detector	Ghosting artifact (Y/N)
a	50	0.5	No	N
b	75	16.0	Pb glass	N
c	50	0.5	No	N

Tolerance:

If no evidence of ghosting is found from visual inspection of the images then the test is passed and there is no need to perform ROI analysis.

Pass/Fail: Pass

4. Sensitivity index consistency

Purpose: To assess the variation of sensitivity between exposure, and set a baseline for monitoring system sensitivity for future QA testing.

Method:

1. Remove grid from system.
2. Expose the entire area of the detector at 75 kVp with 1.5 mmCu. SID to deliver a dose of 1 µGy, 4 µGy, 10 µGy, 12 µGy and 50 µGy.
3. Record the organ program, LUT name and sensitivity index, without changing the window and levelling.
4. Repeat exposure 3 times.

Result:

Table 4: Show relationship between exposure index and dose

Dose (µGy)	EI				STD DEV.	C.V.
	1	2	3	Avg. EI		
1	123.71	122.82	122.82	123.10	0.51	0.0040
4	499.29	500.18	499.74	499.70	0.45	0.0008
10	1258.91	1258.91	1259.80	1259.20	0.51	0.0004
12	1574.86	1575.31	1576.20	1575.50	0.69	0.0004
50	6299.00	6332.82	6325.70	6319.20	17.83	0.0028

Tolerance:

The indicated sensitivity index should not differ by greater than 20% of equivalent exposure, between exposures. The measurement should be used to set a baseline for future QA tests.

Pass/Fail: **Pass**

5. Uniformity

Purpose: To assess the uniformity of the recorded signal from a uniformly exposed detector. A non-uniform response could affect clinical image quality.

Method:

1. Remove grid from system.
2. Expose the entire area of the detector at 75 kVp with 1.5 mmCu. to deliver a dose of 1μGy.
3. Also repeat for 4 μGy, 10 μGy, 12 μGy and 50 μGy.
4. The five values obtained from ROI analysis should be used to calculate five indicated receptor dose values.

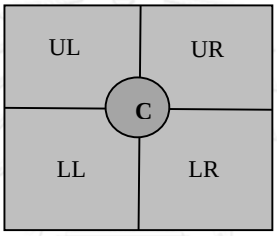

Figure 8: Position of the ROI for uniformity test

Result:

Table 5: The values obtained from ROI analysis and coefficient of variation (CV)

1 μGy	**C=Center**	**UL**	**UR**	**LL**	**LR**	**Avg.**	**STD DEV.**	**CV**
Mean	266.07	285.64	276.71	293.81	285.80	**281.61**	**10.58**	**0.04**
STD Dev.	4.78	5.58	5.36	5.80	5.51			
4μGy	**C=Center**	**UL**	**UR**	**LL**	**LR**	**Avg.**	**STD DEV.**	**CV**
Mean	1087.99	1170.30	1122.68	1194.60	285.80	**1145.61**	**41.54**	**0.04**
STD Dev.	9.44	11.62	10.81	12.50	11.62			
10μGy	**C=Center**	**UL**	**UR**	**LL**	**LR**	**Avg.**	**STD DEV.**	**CV**
Mean	2742.00	2943.70	2812.57	3002.11	2904.83	**2881.04**	**103.89**	**0.04**
STD Dev.	16.40	21.64	19.20	22.54	20.89			
12μGy	**C=Center**	**UL**	**UR**	**LL**	**LR**	**Avg.**	**STD DEV.**	**CV**
Mean	3431.91	3677.63	3535.29	3764.53	3622.21	**3606.31**	**128.29**	**0.04**
STD Dev.	18.55	24.75	22.09	28.41	24.63			
50μGy	**C=Center**	**UL**	**UR**	**LL**	**LR**	**Avg.**	**STD DEV.**	**CV**
Mean	13761.62	14798.78	14113.54	15088.28	14556.37	**14463.72**	**530.68**	**0.04**
STD Dev.	46.85	79.84	65.56	92.06	73.80			

Tolerance:

The images should not have obvious artifacts. Using ROI analysis, STP corrected values should be within a range of 10% of the mean.

Pass/Fail: **Pass**

6. Scaling errors

Purpose: To assess the accuracy of software distance indicators and check for distortion.

Method:

1. Remove grid from system.
2. Position the M1 test object direct onto the detector with an SID of 180 cm.
3. Exposure the detector at 50 kVp 10 mAs with no attenuation in the beam.
4. Using the distance measuring software tools measure the dimensions (x and y) in both the horizontal and vertical directions. Calculate the aspect ratio x/y.

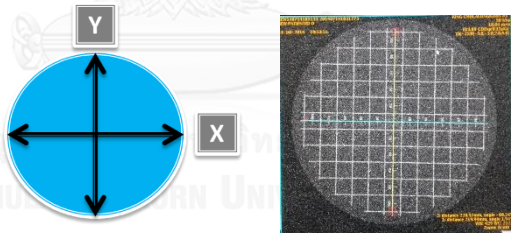

Figure 9: Show scaling error test and software tools measurement

Result:

M1 Object at center 220 mm.

Table 6: The distanced x, y and % different

kVp	mAs	x axis (mm)	y axis (mm)	% different x	% different y	x:y	1-x:y
50	10	219.94	220.37	0.03	0.17	0.980	0.02

Tolerance:

The measured distances x and y should agree within 3% of the actual distances at the center or 5% at the corners. All calculated aspect ratios should be within 1.00 ± 0.03 at the center or 5% at the corners.

Pass/Fail: **Pass**

7. Blurring and stitching artifacts

Purpose: To test for any localized distortion or blurring and to highlight any stitching artifact if the system is formed from more than one detector element.

Method:

1. The test should be made with the grid both in and out of the detector. (this practicum remove grid reduce affect from grid)
2. There is no attenuation in the beam and that the SID is set as 180 cm.
3. With a contact mesh on the detector, exposure 50 kVp 10 mAs using fine focus.
4. Visually inspect the image for blurring and stitching artifacts.
5. Repeat with a finer mesh.

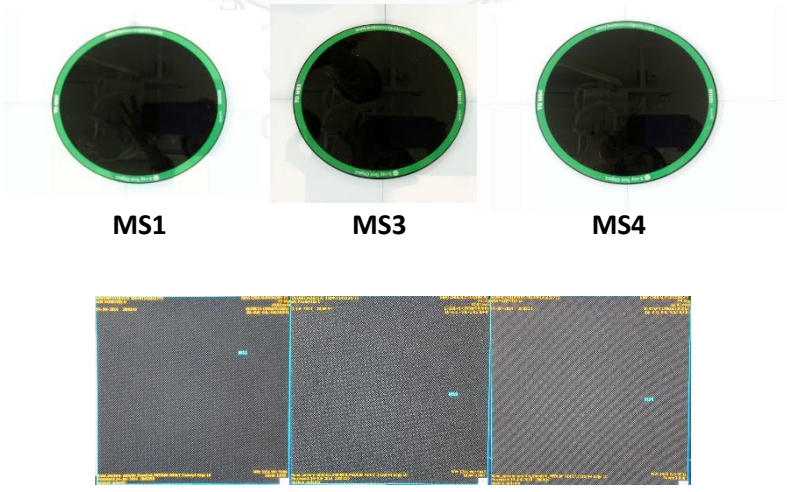

Figure 10: Show MS1, MS3, MS4 test tools and image

Result:

Table 7: Blur area and Stitching obtained images from MS1, MS3 and MS4

Object	kVp	mAs	Blur area(Y/N)	Stitching(Y/N)
MS1	75	10	N	Y
MS3	75	10	N	Y
MS4	75	10	N	Y

Tolerance:

No blurring should be present. If stitching artifacts are present there should be no loss of information.

Pass/Fail: Pass

8. Limiting Spatial Resolution

Purpose: To test the high contrast limit of the system ability to resolve details.

Method:

1. Remove grid from system, there is no attenuation in the beam and that the SID is set as 180 cm.
2. Place the resolution test object Huttner test object onto the detector aligned at 45^{o} to its edges.
3. Exposure the detector at 75 kVp 16 mAs on fine focus.
4. Repeat the measurement with the resolution test object placed at longitudinal axis and -45^{o} to longitudinal axis.
5. Adjust the window level and magnification to optimize the resolution.

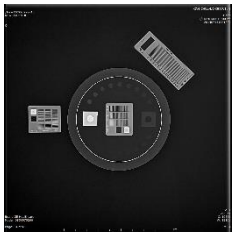

Figure 10: Show image of Huttner test object in 0^{o}, 45^{o} and 90^{o}

Result:

Table 8: Group Line pair in 0°, 45° and 90°

Alignment	kVp	mAs	Line pair Tech monitor (group no.)
0 deg	75	16	6
45 deg	75	16	6
90 deg	75	16	7

Tolerance:

These measurements should be used to set a baseline for future QA tests.

9. Threshold Contrast Detail Detectability

Purpose: To monitor image quality by assessing the visibility of low contrast details.

Method:

1. Remove grid from system.
2. Position the TO20 test object direct onto the detector with an SID of 150 cm.
3. Exposure the detector at 75 kVp and 4 mAs, 1.5 mmCu (Dose 1 µGy).
4. Repeat this test for exposures of 4 µGy, 10 µGy, 12 µGy and 50 µGy.

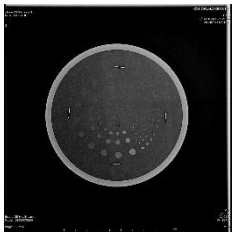

Figure 11: Obtained image form TO20 test tool.

Result:

Table 9: Number of object in threshold contrast detail detectability

Dose(μGy)	kVp	mAs	No. of object low contrast
1	75	4	3
4	75	16	30
10	75	40	33
12	75	50	39
50	75	200	62

Tolerance:

The results of this test are used to set a baseline for future QA tests.

The summary result:

P **1.** Dosimetry
P **2.** Linearity and system transfer properties
P **3.** Image retention
P **4.** Sensitivity index consistency
P **5.** Uniformity
P **6.** Scaling errors
P **7.** Blurring and stitching artifacts
P **8.** Limiting spatial resolution
P **9.** Threshold contrast detail detectability

Appendix C: Case record form

Form 1: Phantom study

Mobile x-ray: **GE-Optima XR220amx No.3**
Image receptor: **GE-DR detector No.3**

• **Phantom Information:**			
Model: **N1-LUNGMAN**		Thickness: **23 cm**	
Exposure parameter:		**Technical parameter:**	
kVp:		FID:	**100 cm**
mAs:		Grid:	**Not use**

• **Radiation dose**	
Entrance Surface Air Kerma (ESAK)	**mGy**

• **Image quality**	
A. Image criteria (CEC)	**Score**
1. Visually sharp reproduction of the vascular of the lungs, particularly the peripheral vessels.	
2. Visually sharp reproduction of the trachea and proximal bronchi.	
3. Visually sharp reproduction of the borders of the heart and the aorta.	
4. Visually sharp reproduction of the diaphragm and lateral costophrenic angles.	
5. Visualization of the retrocardiac lung and the mediastinum.	
6. Visualization of the spine through the heart shadow.	
Total	
Rate of image criteria score: 1 = fulfilled; 0.5 = partly fulfilled; 0 = not fulfilled	
B. Qualitative noise	
Rate of qualitative noise score: 3 = free of noise; 2 = scarce noise; 1 = significant noise; 0 = obvious noise	

Form 2: Patient study

Mobile x-ray: **GE-Optima XR220amx No.3**
Image receptor: **GE-DR detector No.3**

• **Patient Information:**			
Case number:			
Chest thickness: **cm**		Gender (M/F):	
Exposure parameter:		**Technical parameter:**	
kVp:	**90**	FID:	**100 cm**
mAs:	**0.63**	Grid:	**Not use**

• **Patient dose**	
Entrance Surface Air Kerma (ESAK):	**mGy**

• **Image quality**		
A. Image criteria (CEC)		**Score**
1. Visually sharp reproduction of the vascular of the lungs, particularly the peripheral vessels.		
2. Visually sharp reproduction of the trachea and proximal bronchi.		
3. Visually sharp reproduction of the borders of the heart and the aorta.		
4. Visually sharp reproduction of the diaphragm and lateral costophrenic angles.		
5. Visualization of the retrocardiac lung and the mediastinum.		
6. Visualization of the spine through the heart shadow.		
Total		
Rate of image criteria score: 1 = fulfilled; 0.5 = partly fulfilled; 0 = not fulfilled		
B. Qualitative noise		
Rate of qualitative noise score: 3 = free of noise; 2 = scarce noise; 1 = significant noise; 0 = obvious noise		
C. Acceptable of image quality	**Yes**	**No**
Acceptance level: Image criteria score ≥ 3 , Qualitative noise score ≥ 2		

VITA

NAME: Mr.Piyatas Sangdao

SEX: Male

NATIONALITY: Thai

DATE OF BIRTH: 2 December 1970

PLACE OF BIRTH: Bangkok, Thailand

EDUCATION:

1. B.Sc. (Health Education), Rajanagarindra Rajabhat University, 2001
2. B.Sc. (Radiological Technology), Ramkhamhaeng University, 2004

POSITION: Radiological Technologist, Department of Radiology,
Queen Savang Vadhana Memorial Hospital,
Thai Red Cross Society. (1991-Present)

ADDRESS: 97/2 M.1 Nongkham, Sriracha, Chonburi, 20230

E-mail: xray1266@gmail.com

ACADEMIC PUBLICATION

1. Sangdao, P., Krisanachinda, A. and Khamwan, K. Optimization of radiation dose and image quality in chest radiography using digital mobile x-ray system at King Chulalongkorn Memorial Hospital. In proceeding of 14th Asia-Oceania Congress of Medical Physics & 12th South East Asia Congress of Medical Physics. pp. 235-38, Vietnam, 2014.